Masters in Chemical Engineering

Transesterification of Vegetable Oils in Supercritical Fluids for Biodiesel Production

Master's Thesis

Presented by

José Miguel Lopes Maçaira Nogueira

Developed in the course of Dissertation

Conducted in

ETSEIB: Escola Tècnica Superior d'Enginyeria Industrial de Barcelona

FEUP's evaluator: Dra. Conceição Alvim Ferraz

Foreign Institution's tutor: **Dra. Maria Angels Larrayoz**

Chemical Engineering Department

July 2010

Acknowledgments

In this section I would like to express my gratitude to everyone that , one way or another, contributed to the success of this project.

First of all to the Erasmus program and University of Porto for giving young students the amazing experience for studying or working in a foreign institution. It is something that everyone should have the opportunity to do.

To Prof. Maria Angels Larrayoz for the opportunity that gave me, and for the guidance and the knowledge that passed throughout all the project. To Prof. Frances Recasens, head of the research group, that was always available when I needed. To my laboratory colleagues Aline Santana and Adriana Costa that have proportionate so very good work conditions and ambient. To Miguel, Aaron, Edrisi, Sandra and Miguel Dias for all good moments we passed during these months in Barcelona.

To the mechanical workshop of ESTEIB for their exceptional work and skills, that helped me in every situation needed in the assembling of the experimental apparatus. To Israel, from Shimadzu, for the chromatography knowledge that he transmitted me.

To all my friend that also were in the Erasmus program or in Portugal, João Mendes, André Maia, Sara, Marta, Chaves, Paula, Tó, Mj, Ruca and Catarina. It was a fantastic five years period.

To my friends in Espinho, Luis Diogo, Miguel, Hugo and Jonathan..for the good moments I know we will spend when I get back.

To the best landlords in the world, Cristiana and Reynaldo. A huge thanks for everything, for all the amazing moments we spent together, and for the help you gave me. Family will come first always.

To my girlfriend Erica, that besides the distance always supported me. Thank you for all the moments we've spent together. "Without you it would not have been the same"

To all my family, in particular to my parents and brother. Without you I would not be the person I am today. Thank you for all the education and the values you passed on to me.

Thank you all!

Abstract

In this work, the main objective was the continuous production of biodiesel using a solid acid catalyst under supercritical conditions. This was done by using refined synthetic oil, with similar composition to sunflower oil. Biodiesel is becoming an inevitable part of sustainable economy and has emerged as one of the most potential renewable energy sources to replace current petrol-derived diesel.

A complete setup, to conduct the transesterification reaction of the synthetic oil with methanol, in continuous mode, was designed and assembled. The main piece of equipment was a titanium fixed bed reactor. The experimental setup is prepared to work in harsh conditions with temperatures up to 200ºC and pressures up to 300 bar. The heterogeneous catalyst used was a silica-supported sulfonic acid polymer, Nafion® SAC-13.

In order to determine the operating conditions of the reactor, a preliminary thermodynamic study was made to determine the critical temperature and pressure of the reaction mixture. The reaction was conducted using carbon dioxide as co-solvent with the objective of reducing the critical properties of the system, so a heterogeneous catalyst could be employed. The reaction was carried out at 250 bar with temperatures varying from 150ºC to 205ºC. By varying the inlet mixture flow rate, and thus the space time, several experiments were conducted at three temperatures allowing the determination of the observed reaction rate and the activation energy for the reaction. Using several correlations available in literature, the mass transfer coefficients were determined, and it was concluded that there were no mass transfer limitations between the fluid phase and the solid catalyst.

The reaction rate constants were determined using two different kinetic approaches: considering one step irreversible reaction and three step reversible reaction schemes. In this last case, the calculation of the reaction rate constants needed the integration and resolution of a differential equation system. A mathematical program was written and used to simulate the equation system and to adjust the kinetic model to the experimental points. The estimated reaction rate constants indicate an Arrhenius dependence on temperature. For the transesterification of the synthetic oil, the highest value of fatty acid methyl esters (in mass percentage) was achieved at the highest temperature, 205ºC, where nearly complete conversion of triglycerides (99.3%) originated 82% of FAMEs in only 2 minutes of space time in the reactor.

The production of biodiesel was conducted in conditions that, so far the completion of this project, were not reported. The transesterification of synthetic oil in supercritical conditions, using a solid catalyst, in the presence of carbon dioxide as co-solvent lead to high reaction rates and almost complete conversion of triglycerides in very short space times, thus offering a promising route for the investigation of biodiesel production.

Table of Contents

List of Figures

List of Tables

1 Introduction

1.1 Relevance and Motivation

Biofuels have become a major issue in the last years all over the world, especially because the recent rising in the oil prices, but also because the growing of the public awareness related to the energy and environmental issues. The fossil fuels produced from petroleum, like gasoline and diesel, come in the category of non-renewable fuel, and will last for a limited period of time. The World Energy Forum predicted that fossil oil will be exhausted in less than 10 decades, if new oil wells are not found [(1)]. Figure 1 presents the projection of energy demand for the new future, indicating that there is an urgent need to find more renewable energies sources to assure energy security worldwide [(2)].

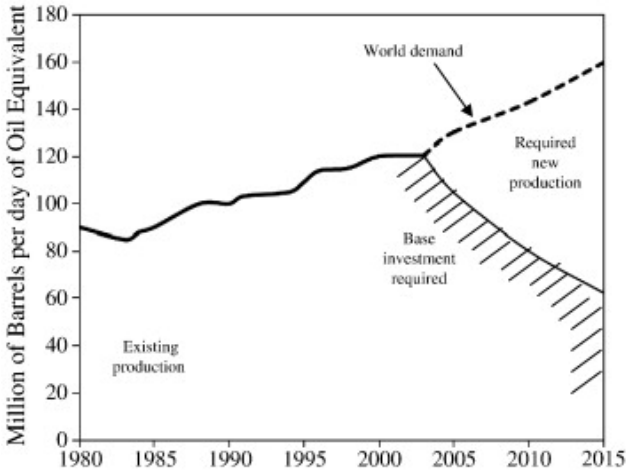

Figure 1: Projection of energy demands for the new future

Renewable energy has been gaining importance in the last ten years due to its potential to replace fossil fuel, particularly in transportation. These sources such as wind energy, solar energy, hydro energy, and energy from biomass have been successfully developed and used worldwide in order to decrease the dependence on fossil fuels. However, according to the International Energy Agency (IEA), the energy produced from renewable combustibles and waste have the highest potential among the other renewable sources. As shown in Figure 2 combustible renewable energy sources account for 10%, more than hydro and others (includes geothermal, solar, wind and heat) [(2)]. So it is predicted that renewable energy from combustible energies, such as bio fuels, will enter the market intensively in the next years in order to diversify the global sources of energy.

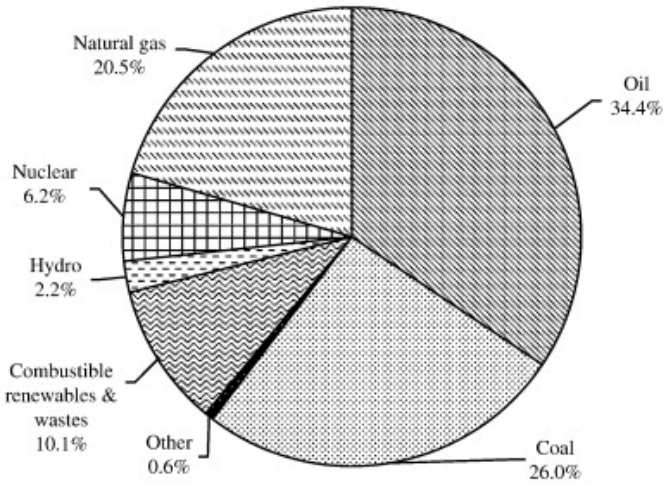

Figure 2: World total energy supply by fuel in year 2006 (excluding electricity and heat thread). Total 11,741 million tones of oil equivalent (Mtoe)

The use and production of non-renewable fuels also emit pollutants in the form of oxides of nitrogen, oxides of sulphur, carbon dioxide, carbon monoxide, lead, hydrocarbons, etc. The need of a supplement and eventually for a substitute for these fuels is more urgent than ever, and bio fuels will probably be part of the solution.

The bio fuel that has been more successful in fuel engines is the so called "biodiesel" or fatty methyl esters. The reason that biodiesel has become the leading bio fuel is due to the similar fuel properties that has, comparing to fossil fuel. It also can be used without any changes to the engine, which makes it acceptable by the engine manufacturers. Another reason that explains the quick market penetration of this product is the relatively ease in its production, as it can be produced both in small scale and industrial scale, and also the variety of feedstocks that can be used for its production. Comparing directly biodiesel with petroleum-based fuels one can find several advantages in most technical aspects:

- Derivation form a renewable resource, thus reducing dependence on petroleum;
- Biodegradability;
- Reduction of most exhaust emissions (with the exception of nitrogen oxides, NO_x);
- Higher flash-point, leading to safer handling and storage;
- Excellent lubricity, a fact that is steadily gaining importance with the advent of low-sulfur petro diesel fuels, which have greatly reduced lubricity. It has been reported that adding biodiesel at low levels (1-2%) restores the lubricity [(3)]

One of the leading regions for the production of biodiesel is Europe, where the first pilot plant for its production was installed in Austria in 1987. The possibility of using pure biodiesel without paying mineral tax has led to the installation of several industrial scale plants in 1991 in Austria and Germany, but soon other countries like Italy France and the Czech Republic followed. The development of biodiesel activities increased abruptly when in the year 2003,

the European directive for the promotion of biodiesel [4] demanded a market share of biodiesel of 5.75% for the transport fuel in 2010. Figure 3 shows this evolution of the biodiesel production by the European countries.

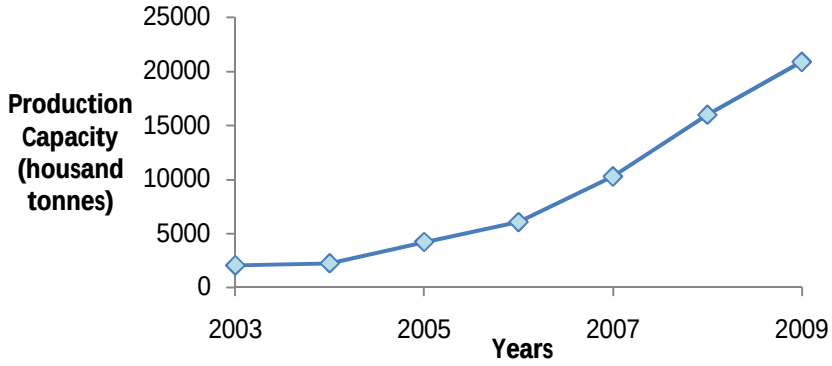

Figure 3: Evolution of the production capacity of Biodiesel of the E.U. countries [5]

In 2009 a new directive [6] states a demand of 20% share of energy from renewable sources and a 10% share of energy from renewable sources in transport in community energy consumption by 2010. An overview of the Europeean production of biodiesel is presented in Table 1.

Table 1: E.U. biodiesel Production in 2009, in 1000 tons [5]

Country	Production in 1000 tons	Country	Production in 1000 tons
Austria	707	Italy*	1,910
Belgium	705	Latvia	136
Bulgaria	435	Lithuania	147
Cyprus	20	Luxemburg	0
Czech Republic	325	Malta	8
Denmark	140	The Netherlands	1,036
Estonia	135	Poland	580
Finland*	340	Portugal	468
France	2,505	Romania	307
Germany	5,200	Slovakia	247
Greece	715	Slovenia	100
Hungary	186	Spain	3,656
Ireland*	80	Sweden	212
Total			**20,909**

The 2009 production was increased by 35,7% compared to 2008, and is expected to continue to increase. This explosion in biodiesel production is believed to be cooled down by the lack of raw materials which have to be, in the majority of cases, imported. [5]

The production of biodiesel is now spread worldwide, being more intensive in countries which are also those with the largest production of vegetable oils, such as Malaysia and India or Brazil and Argentina.

Today an estimated production of 30 million tons of biodiesel exists worldwide. On the other hand there is a total annual production of vegetable oils of approximately 100 million tons [(7)]. A big percentage of this value is for food purposes, which lead to an inevitable competition between the food market and the bio fuel industry. Although the achievements of agriculture and plant cultivation have made it possible to exceed the demand resulting from world population, the production of vegetable oil cannot be increased to the demand of biodiesel because it would led to an unsustainable production of oil plants. The concern for this unsustainable production has led the society to extensive discussions, making the search for non-edible sources of oil a research area.

Feedstocks for Biodiesel Production

The major vegetable oil seeds and fruits utilized for edible purposes are listed in Appendix A, with their typical oil contents, yield per acre of land and major producing areas. [(8)]

All vegetable oils and animal fats are potential feed stocks for the biodiesel production, as they have similar chemical composition. The chemical and physical properties of fats and oils are largely determined by the fatty acids that they contain and their position within the triacylglycerol molecule. Chemically all fats and oils are esters of glycerine and fatty acids; nevertheless, the physical properties of natural fats and oils vary widely because: the proportions of fatty acids vary over a wide range; the triaglycerol structures vary for each individual oil and fat.

Fat and oils are commonly referred to as triglycerides because the glycerin molecule has three hydroxyl groups where a fatty acid can be attached. All triglycerides have the same glycerin unit, so it is the fatty acids that are attached to it that determine its properties. The fatty acid components are distinguished in three ways: chain length; number and position of the double bonds; and the position of the fatty acids within the glycerine molecule.

The difference in chemical and physical properties between the existing variety of edible oils and fats are explained by variations in these three characteristics.

The structure of a fatty acid is commonly denoted by the name of its parent hydrocarbon, by its common name, or by a convenient shorthand designation showing the number of carbon atoms and the number of double bonds, followed by a systematic name. The fatty acid carbon chain lengths vary between 4 and 24 carbon atoms with up to three double bonds. The most prevalent saturated fatty acids are lauric (C-12:0), myristic (C-14:0), palmitic (C-16:0), stearic (C-18:0), arachidic (C-20:0), behenic (C-22:0), and lignoceric (C-24:0). The

most important monosanturated fatty acids are oleic (C-18:1) and erucic(C-22:1). The essential polyunsaturated fatty acids are linoleic (C-18:2) and linolenic (C-18:3) [8].

The fatty acid compositions of natural fats and oils vary significantly depending not only on the plant or animal species but also within the same species. Among the factors that affect the vegetable oil fatty acid compositions are climate conditions, soil type, growing season, plant maturity, plant health, microbiological conditions, seed location within the flower, and genetic variation of the plant. Animal fat and oil composition varies according to the animal species, diet, health, fat location on the carcass, and maturity. [9] The different fatty acids that are contained in the triglyceride comprise the fatty acid profile (or fatty acid composition) of the vegetable oil or animal fat. Because different fatty acids have different physical and chemical properties, the fatty acid profile is probably the most important parameter influencing the corresponding properties of a vegetable oil or animal fat.

Principles for Biodiesel Production

Fatty acid methyl esters have been known for over 150 years. The first description of the preparation of the esters was published in 1852. However, for a long time fatty acid methyl esters were mainly used as derivatives for analyzing the fatty acid distribution of fats and oils, so the preparation mainly was done in analytical scale. Since the mid 20th century fatty acid methyl esters have become a major oleo chemical commodity as intermediate for the production of fatty alcohols, used for the production of non-ionic detergents. But only since the late Seventies have fatty acid methyl esters have been tested and used as diesel fuel substitute. [7]

Chemically biodiesel is equivalent to fatty acid methyl esters or ethyl esters produced out of triacylglycerols via transesterification or out of fatty acids via esterification. Methyl esters or ethyl esters produced from fatty acids have similar combustion characteristics in diesel engines, because the major components in fossil diesel fuel are also straight chain hydrocarbons with a chain length of about 16 carbons (hexadecane, 'cetane') [3] .

The reactions associated most commonly to biodiesel production include transesterification and esterification, but with potential competing reactions including hydrolysis and saponification. [10].

In Figure 4 the scheme for the production of mono alkyl esters form triacylglycerol is shown. Fatty acid methyl esters today are the most commonly used biodiesel species, whereas fatty acid ethyl esters (FAEE) so far have been only produced in laboratory or pilot scale.

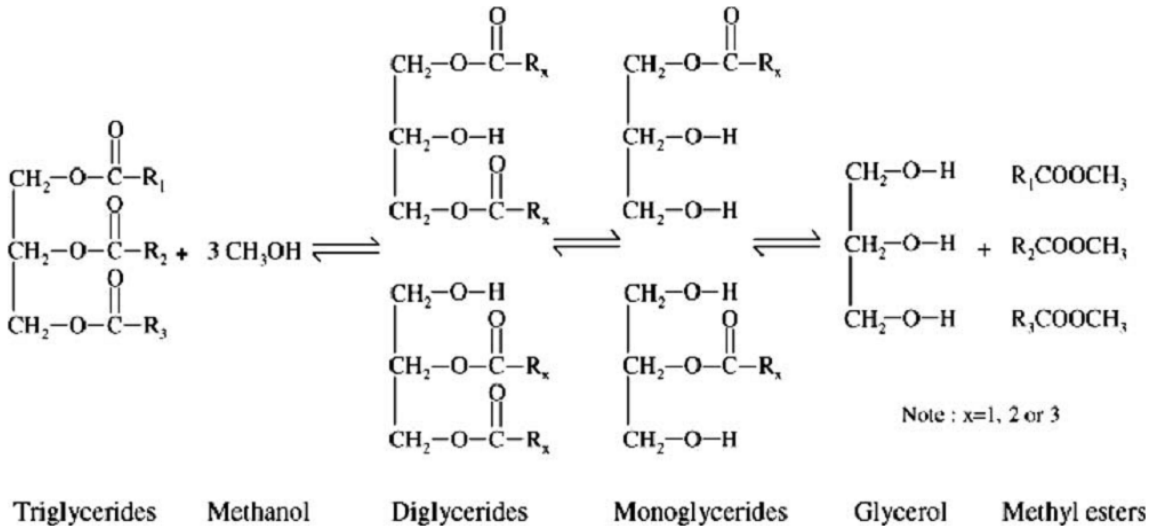

Figure 4: Production of fatty acid mono alkyl esters via transesterification [11]

In a transesterification or alcoholysis reaction one mole of triglyceride reacts with three moles of alcohol to form one mole of glycerol and three moles of the respective fatty acid alkyl ester. The process is a sequence of three reversible reactions, in which the triglyceride molecule is converted step by step into diglyceride, monoglyceride and glycerol. In order to shift the equilibrium to the right, methanol is added in an excess over the stoichiometric amount in most commercial biodiesel production plants. A main advantage of methanolysis as compared to transesterification with higher alcohols is the fact that the two main products, glycerol and fatty acid methyl esters (FAME), are hardly miscible and thus form separate phases – an upper ester phase and a lower glycerol phase. This process removes glycerol from the reaction mixture and enables high conversion. Ester yields can even be increased – while at the same time minimizing the excess amount of methanol – by conducting methanolysis in two or three steps. Here only a portion of the total alcohol volume required is added in each step, and the glycerol phase produced is separated after each process stage. Finally, regardless of the type of alcohol used, some form of catalyst has to be present to achieve high ester yields under comparatively mild reaction conditions. [7]

The esterification process is a reversible reaction where free fatty acids (FFA) are converted to alkyl esters via acid catalysis (HCl or more commonly H_2SO_4). When oils are high in free fatty acids as common in waste cooking oils, the simultaneous esterification and transesterification reactions via acid catalysis is advantageous to potentially obtain nearly complete conversion to biodiesel. The esterification process follows a similar reaction mechanism of acid-transesterification. The reactants including FFA and alcohol are catalyzed by acid to create the alkyl ester and water .

In Figure 5 is illustrated the schematic course of a typical methanolysis reaction. Whereas the concentration of triglycerides as the starting material decreases and the

amount of methyl esters as the desired product increases throughout the reaction, the concentrations of partial glycerides (i.e. mono- and diglycerides) reach a passing maximum.

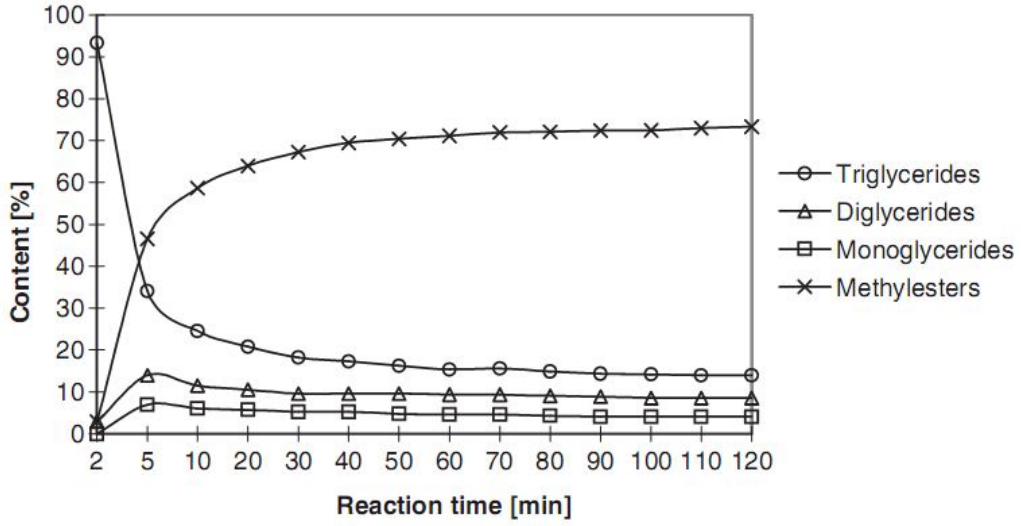

Figure 5: Schematic course of a typical methanolysis reaction (adapted from [7]). Reaction conditions: sunflower oil: methanol molar ratio = 3:1, 0.5% KOH, T=25ºC

The transesterification reaction according to the above picture is a typical equilibrium reaction, so to increase the yield of fatty acid alkyl esters it is necessary to use an excess of alcohol or to remove one of the end products out of the equilibrium, e.g. the water by distillation or by the use of concentrated sulphuric acid. In order to increase the reaction rate of transesterification or esterification in most cases catalysts are used.

1.2 Objectives and Outline

As been discussed, several techniques can be employed for the production of biodiesel. The most widespread today make use of homogeneous catalyst, in batch or in continuous-flow environments. Both reaction and separation steps can create bottlenecks.

The availability of heterogeneous catalysis allows the suppression of neutralization and washing steps, leading to a simpler and more efficient process. However, the research of super active and robust catalysts is still an open problem. Supercritical hydrolysis and transesterification can be conducted without a catalyst, but in extreme conditions of pressure and temperature.

The objective of this thesis is to combine these conventional techniques to a continuous process of biodiesel production. The main objective is to produce biodiesel in continuous mode, using a solid catalyst in supercritical conditions. To accomplish this objective several steps are necessary:

- A preliminary thermodynamic study to assess the critical properties of the reaction mixture. A co-solvent (carbon dioxide) is added to decrease the critical temperature and pressure of the mixture methanol/oil to allow the usage of a solid catalyst (Nafion SAC®-13). The minimum operating conditions were 150ºC and 250 bar.
- The design, assemble and operation of a continuous experimental setup for the production of biodiesel. This was done by using a titanium fixed bed reactor.
- Determination, by gas chromatography, the fatty acid methyl esters (FAMEs), and glycerides (glycerol,mono-,di-, and triglycerides) content in the produced samples.
- Choosing an appropriate kinetic model to assess the reaction rate constants and activation energies. For this a Matlab (The Math works Inc.) was used to resolve the differential equation system and to adjust the kinetic model parameters to the experimental points.

This work is divided into seven main chapters. Chapter 1 is a brief introduction, pointing out the relevance and motivation of the work. Chapter 2 describers the basic principles in the current status of the production of biodiesel. Chapter 3 describes all the work done regarding the assembling the experimental apparatus. Chapter 4 contains the preliminary thermodynamic study made for the determination of the operating conditions of the reactor. Chapter 5 introduces the transesterification reaction conducted, and Chapter 6 contains the results obtained. In chapter 7 are presented the conclusions drawn from this work and some suggestions for future work.

2 State of the Art

Older biodiesel processes are essentially batchwise. The oil is submitted to transesterification in a stirred- tank reactor in the presence of a large amount of methanol, and base catalyst, mostly NaOH or KOH. An excess of methanol is necessary chiefly to ensure full solubility of triglyceride and keep the viscosity of the reaction mixture low, but also for shifting the chemical equilibrium. A minimum molar ratio methanol:triglyceride of 6:1 is generally accepted [(12)].The reaction takes place at temperatures from 60 to 80° C, slightly below the mixture boiling point at the operating pressure. Previously, the oil should be neutralized by treatment with aqueous sodium hydroxide for the removal of free fatty acids. These can be found between 0.5 and 5% in the vegetable oils, somewhat more in animal fats,

but can rise to up to 30% in used cooking oil. High FFA content needs special pretreatment by esterification. The transesterification reaction may be considered finished when the conversion reaches 98.5%. However, the mixture composition should respect the quality biodiesel specifications. The excess methanol is recovered for the next batch. The remaining mixture is submitted to the separation of esters from glycerol. This can take place either by decantation or by centrifugation.

Water may be added to improve the phase split. The oil phase containing fatty esters is sent to finishing by neutralization with acid, followed by washing and drying. Phosphoric acid is frequently for neutralization used since $Na_3\ PO_4$ or $K_3\ PO_4$ can be recovered and sold as fertilizers. The water phase from washing is returned to glycerol separation. [12]

After mixing of glycerol streams the result is about 50% glycerol– water solution with some methanol, residual base catalyst and soaps. Firstly, the methanol recovery takes place by flash distillation or film evaporation. Then, by adding acid the soaps are transformed in free fatty acids, which separate from glycerol as a top oily phase. Next, the FFA can be recovered and valorized by esterification with methanol. Finally the glycerol should have a purity of about 85% and be sold to specialized refiners. Purity of 99.5–99.7% can be achieved by applying vacuum distillation or ion- exchange process. [7]

The batch process allows high flexibility with respect to the composition of the feedstock. In turn, the economic indices are on the lower side because of lower equipment productivity and higher operation costs, such as manpower and automation. The use of a large excess of methanol is reflected in higher energy consumption if no heat- integration measures are taken. Large amounts of wastewater formed by acid- base neutralization need costly treatment.

The productivity can be greatly improved by the implementation of continuous operations and the use of process- intensification techniques, such as reactive distillation [3]. The replacement of a homogeneous catalyst by a heterogeneous one is highly desirable.

The replacement of homogeneous catalysis by solid catalysts brings obvious economical and technological advantages. For this reason, a considerable research effort is being devoted in this area.

A first application regards the esterification reaction. Here, solid catalysts with acidic character can be used, such as zeolites, ion- exchange resins, sulfated metal oxides, sulfated carbon fibers, etc. However, only few are suitable for handling long-chain complex molecules. Some can achieve super acidity comparable with sulfuric acid. Ion-exchange resins, such as Nafion and Amberlyst are capable of achieving high reaction rate at moderate temperatures below 130 °C, but their chemical stability at longer operation seems to raise concerns. On the contrary, sulfated zirconia and tin oxides can be used at higher temperatures, 140 to 180° C, and ensure high reaction rates, but are sensitive to deactivation by sulfur-group leaching if free

water is present. Since the water produced by esterification limits also achieving high conversion because of the chemical equilibrium, a good solution for solving both problems is employing reactive distillation. The second area of heterogeneous catalysis in biodiesel manufacturing is the transesterification reaction. Here again, the base catalysts exhibit typically much higher activity than the acidic ones, but finding effective catalysts is still an open problem. Some solid metal oxides, such as those of tin, magnesium, and zinc could be used directly, but they actually act by a homogeneous mechanism. [13]

Performing the esterification in supercritical conditions has been studied initially as a method to solve the problem of miscibility of oil and methanol that hinders the kinetics in normal conditions. Since the critical coordinates of methanol are 239 °C and 80 bar, raising the temperature and pressures at sufficiently high values is necessary. Studies conducted in Japan [12] demonstrated the feasibility of producing biodiesel by the esterification of rapeseed with methanol without a catalyst working around 350° C and 200 bar at molar ratio methanol:oil of 42: 1 for reaction times below 4min . The advantage of avoiding a catalyst is obvious. However, the conditions of pressure and temperature are severe and need special equipment. Recent research showed the real yield can be reduced by thermal degradation of biodiesel, namely of unsaturated fatty esters [14] .For this reason, lowering the reaction temperature and pressure is highly desirable.

The assessment of the critical region of a mixture triglyceride/methanol can be made by applying the approach explained next. The critical properties of individual triglycerides component can be estimated by a suitable group- contribution method, and then using mixing rules for averaging the parameters function of composition [12]

Table 2 presents the critical values obtained for different molar ratio methanol/oil starting with 6, corresponding to a low solubility limit, and ending with 42, the highest practical value tested in laboratory experiments [15].

Table 2: Critical properties of mixture oi/methanol in differenrt molar ratios R

Properties	Methanol	Coconut Oil	R=6	R=12	R=24	R=42
Critical Temperature, ºC	239.5	606.8	395.9	345.9	305.8	282.2
Critical Pressure, atm	79.9	6.2	37.2	50.3	61.7	68.4
Critical volume, $l.mol^{-1}$	118	2.366	0.33	0.22	0.22	0.22

It can be seen that the critical temperature drops rapidly with increased methanol/oil ratio to about 280° C, while the critical pressure rises up to about 70atm, close to methanol. In practice, operating parameters of 350° C and 190 bar were employed at a residence time of 400s

The addition of co-solvent in combination with supercritical conditions seems to be an efficient means to reduce significantly the operating temperature [16] . For example, soybean oil could be converted with methanol into biodiesel with 98% yield by using propane, at least in 0.05 molar ratio to methanol, at 280° C and 12.8 MPa. Similar results have been reported with CO2 in a molar ratio of 0.1 with respect to methanol. In both cases the optimal ratio methanol/oil was 24 and residence time of 10min [16] .

3 Setup for the continuous production of Biodiesel

The main objective of this work is the continuous production of biodiesel in supercritical conditions using a synthetic vegetable oil, and to assess the influence of the operating conditions in its production. To accomplish this, the first and most important step was the design and construction of a fully operational pilot installation. This chapter describes the work done regarding the construction, mounting and description of the experimental setup. It is prepared to operate in "harsh" conditions, with temperatures up to 250ºC and 300 bar. More description of the installation and its equipment will be given in the following sections.

3.1 General description of the installation

The apparatus built in this work was conceived to work at high values of temperature and pressure, to allow the transesterification of vegetable oil in supercritical conditions. A picture of this setup is shown in Figure 6 and the layout of the installation is presented in Figure 7.

Figure 6: Overview picture taken to the experimental installation

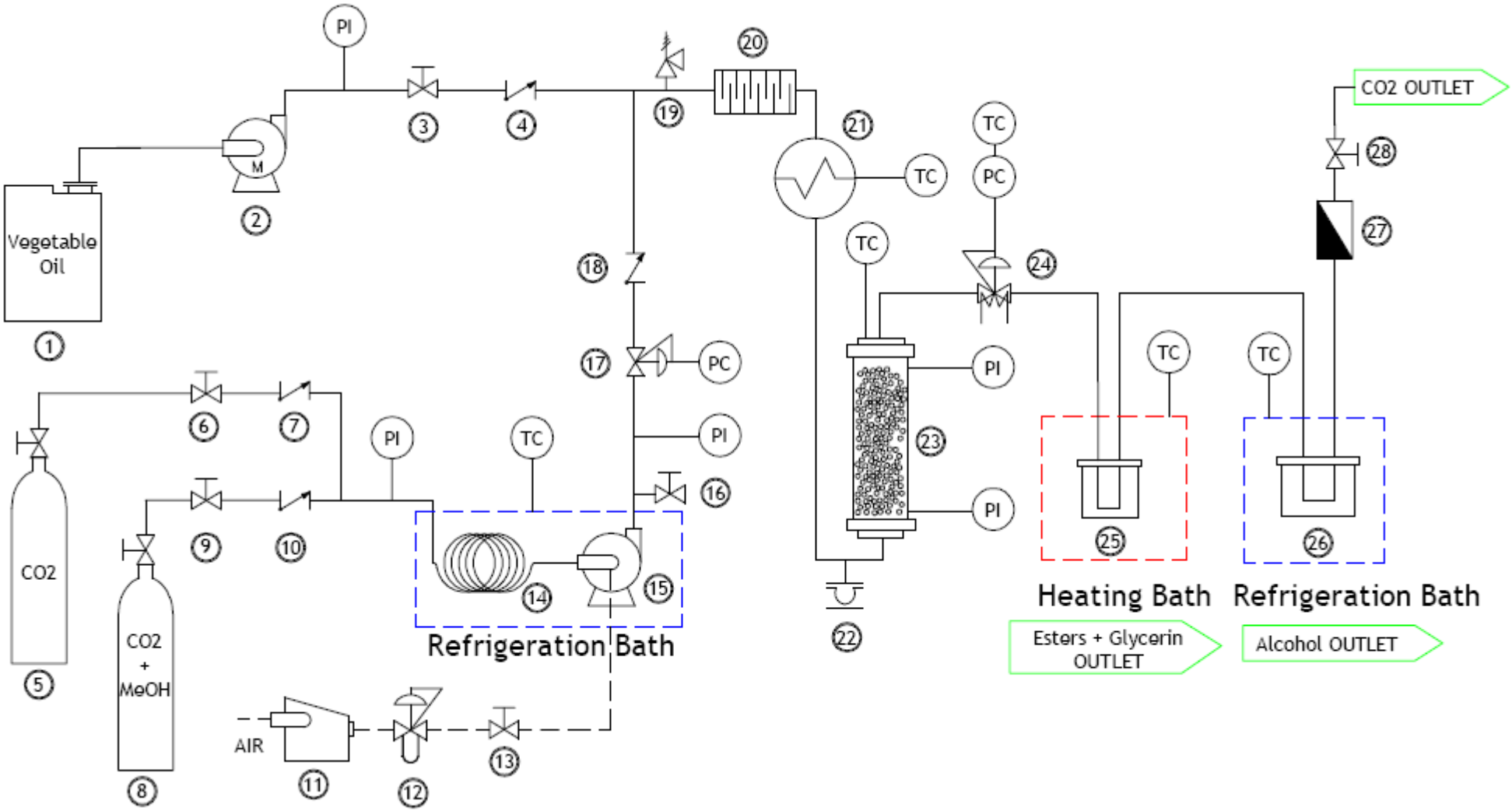

Figure 7: Scheme of the experimental Installation for the continuous production of Biodiesel:
1-Sunflower Oil; 2-Oil piston pump; 3-Line valve; 4-Check valve; 5-CO2 Bottle; 6-Line valve; 7-Check valve; 8-CO2/Methanol mixture bottle; 9-mixture line valve; 10-mixture check valve; 11-Compressor;12-Pressure regulator;13-Line valve;14-Cooling device;15-Mixture pump;16-Purge valve; 17-Pressure regulator;18-Check valve;19-Safety valve;20-Static Mixer;21-Pre-heater; 22-Rupture disk;23-Fixed bed reactor;24-Expansion needle-valve;25-Sample collector;26- Alcohol collector;27-Flowmeter;28-Line valve.

In the layout presented in Figure 7 two major feed lines can be seen corresponding to the vegetable oil, and other to the methanol/carbon dioxide.

Because the installation was intended to be operated at high pressures, a method to ensure that there were no leaks in the equipment had to be performed. This was done by passing gas in all the tubing and equipments of the experimental apparatus. The gas chosen was carbon dioxide, as it is a relative safe, non toxic and not expensive gas.

The starting up of the installation was done using only the carbon dioxide line, so the mixture of alcohol/carbon dioxide could be used only when the intended operating conditions were reached. Depending on the working flow rate this could take several minutes. After each bottle (CO2 and mixture) there are placed two on/off valves, 6 and 9, and two check valves, 7 and 10, used to prevent back flow of the gas. After these two feed lines there is a pressure indicator that is used to monitor the status of each bottle.

Both feed lines are pressurized by pumps: the oil inlet is pressurized by pump 2 (Gilson, HPLC pump model 305), and the methanol/CO_2 mixture is pressurized by an air driven piston pump (Maximator®, model M111D-327, Germany), 12,

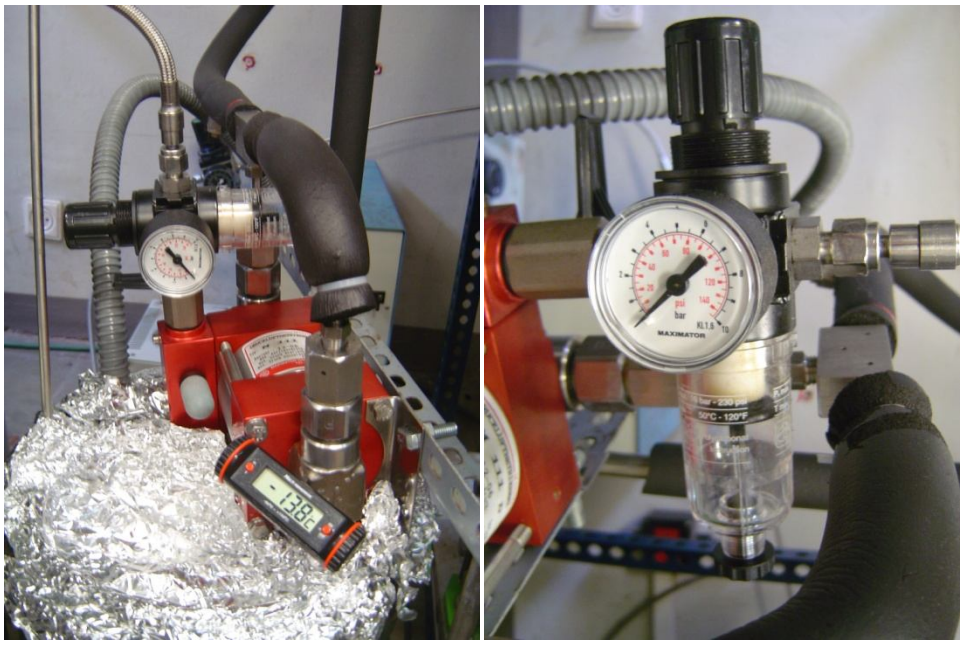

Figure 8: Air driven piston pump, Maximator model M111D-327, used for the pressurization of the mixture stream

The pump is driven by compressed air in the range of 1-10 bar, that is supplied by a compressor (ABAC model B4900LN/T4), represented by 11. The outlet pressure is calculated by the transmission ratio between air piston and plunger piston multiplied by the drive pressure. That is, the static ultimate pressure of the hydraulic can be adjusted of the supply pressure. In this pump model the transmission ratio was 130, so to reach operating pressures of 250bar the drive pressure from the compressor was regulated to about 1,5 bar. This was done by a

compressed air control unit represented by 12 and in Figure 8, that is placed in the air feed line downstream the pump. This compressed air control unit consists of pressure filter, water separator, shut-off valve, pressure controller, pressure gauge and safety valve. The pressure filter and water separator are necessary to ensure that no foreign matter, up to 5 µm of particle size (information given by the manufacturer), or water enters the pump respectively, and thus avoiding malfunctioning and damaging the equipment.

Because the mixture used is contained in a pressurized gas/liquid bottle (Lindle, Germany), the inlet tubing of the piston pump (14) and the pump (15) itself (the suction portion of the pump) are immersed in a temperature controlled bath to ensure that only liquid is fed to the piston pump. The refrigeration bath is controlled to maintain an approximate temperature of -14 ºC. At this temperature both carbon dioxide and methanol are liquid and the mixture can be pressurized and pumped to the installation.

After this pump it was placed a purge valve, 13, that was used to purge the line of any gas bubbles that might be formed inside the tubing. A pressure indicator placed after the pump gives indication of what pressure the pump is pressurizing the inlet feed. A pressure regulator, 14, was placed after the piston pump and the purge valve, to reduce the pressure in upstream this point. This was necessary to prevent excessive pressurization of the equipment upstream the pump.

The other feed line, of vegetable oil, is pressurized by pump 2 (Gilson, HPLC pump model 305) shown in Figure 9, and has a on/off valve to shut and open the feed of oil, and a check valve to prevent that methanol or carbon dioxide enters the pump by the pressure side.

Figure 9: Gilson HPLC pump used for the pressurizing of the vegetable oil

Both feed lines are connected by a "T" type connection and are mixed in a static mixer, 17 (Kenics, model 37-04-065). For security reasons a security valve, 19, is placed before the static mixer, and it is calibrated for 350 bar. If for any reason there is an unexpected rise of pressure, the security valve will open automatically preventing this way damage in the equipments located next to this valve.

The mixture is then heated in a pre-heater, 21, (Kosmon S.A., model 43000) to the intended working temperature before it enters the reactor. In the reactor feed line is placed a rupture disk (22), once more for security reasons, which is calibrated to 350 bar.

The mixture then enters the titanium reactor, 23, (Eurotechnica, HPA 500) where the reaction takes place. The temperature is controlled by two external resistances. The measurements of the temperature are made in the external reactor walls, and also inside the reactor by a thermocouple (type k, stainless steel). Pressure is also measured in the inlet and outlet of the reactor, to check for pressure drops in the fixed bed reactor.

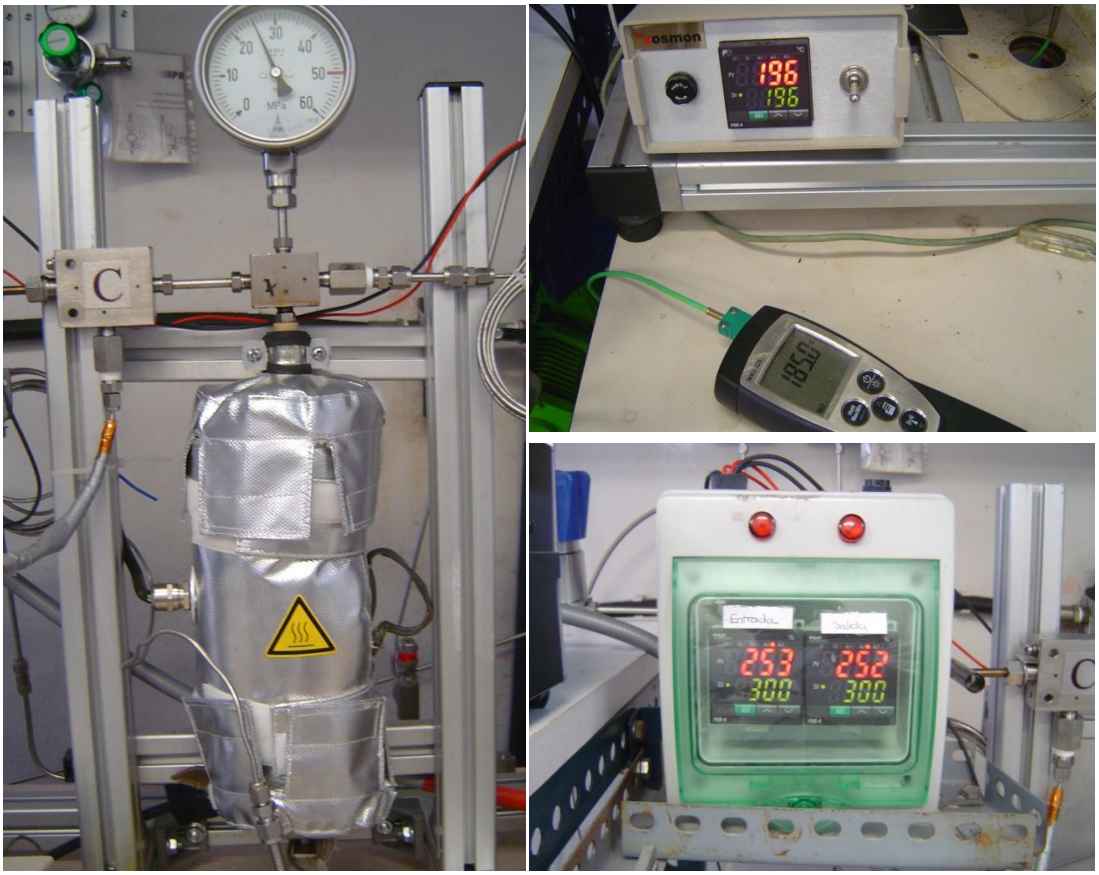

Figure 10: Titanium fixed bed reactor and pressure and temperature indicators

After leaving the reactor the reaction mixture is continuously expanded to atmospheric pressure on an externally heated needle valve (Autoclave Engineers, Erie, PA) in order to control the total flow of the reactor mixture. This valve had to be externally heated due to the expansion of the gas. From 250 bar to atmospheric pressure, there is an enormous decrease in temperature what would cause the valve to freeze and could led to its malfunctioning and damage. The tubing that follows the expansion valve is also heated by an external resistance wire (Kosmon, S.A.) to prevent freezing of the mixture due to the referred gas expansion.

Figure 11: Expansion valve (Autoclave Engineers) with external heating

This effluent was then sent to a glass container, 25, which is immersed in a heated bath in a constant temperature of 70ºC. Here the unreacted methanol is evaporated from the mixture and along with the carbon dioxide is conducted to a series of glass U-tubes, 26, immersed in an ethylene glycol-water (40% v/v) bath held at -10 ºC to condense the methanol from the carbon dioxide. The flow rate of exhaust gas (carbon dioxide) was measured with a CO_2 flow meter (Tecfluid, Spain) and sent to the gas exhaust system.

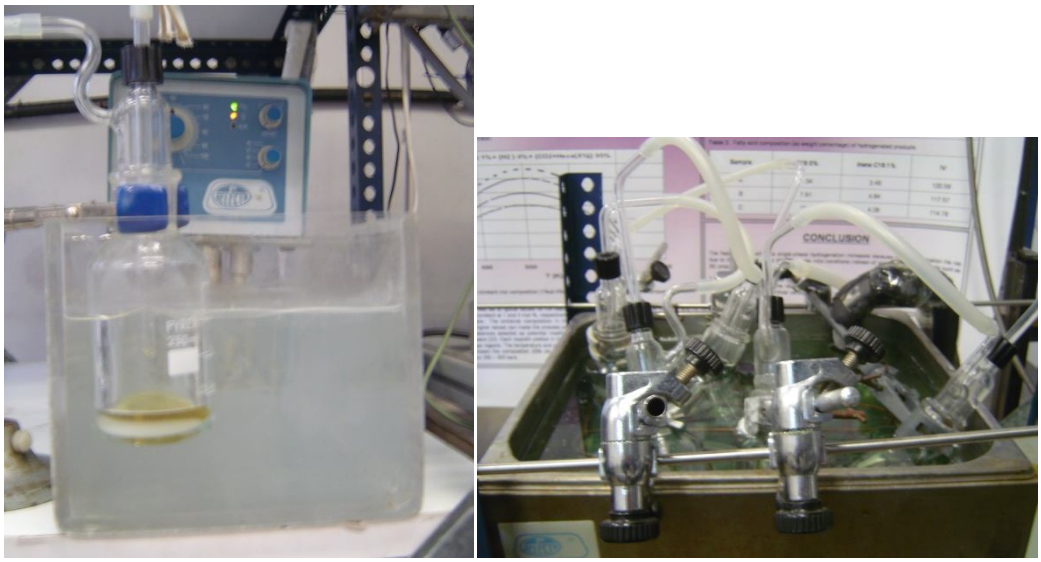

Figure 12: Thermostatic bath used to evaporate the unreacted methanol (left), and ethylene glycol- water bath used to condense the methanol

3.2 System Operation

The first step to operate the described experimental installation was the turning on the temperature controlling baths. The cooling bath that controlled the temperature of the inlet tubing,14, and the suction part of the pump 15, was held approximately at -14 ºC to ensure

that all the gas that passed through the bath and fed to the pump would condensate and be in the liquid phase. Also the bath were the samples of biodiesel were collected and the methanol was evaporated, 25, and the one than condensates the methanol,26, were turned on and held at 70 ºC and -10ºC respectevely. The reactor temperature control was switched on and set to the desired temperature, as well the heating for the expansion valve and the subsequent tubing. The preheater, 21, was also set to the intended working temperature. Because the installation is to operate in a continuous mode, the flow that passes through the reactor has influence on its temperature. So there were always a difference of about 15ºC between the temperature of the wall of the reactor (where the temperature controller is placed) and the real and observed temperature inside the reactor. This difference was more notice when working at higher flow rates.

After all the temperature controlled equipments were switched on, the supply line of carbon dioxide was open and passed through all the installation. The compressor, 11, was started and the pressure regulator, 12 , was set to give the intended supply air pressure to the piston pump. For working at 250 bar , this was set to 2 bar. Then the intended pressure and flow rate inside the reactor were regulated by the pressure regulated 17, and the expansion needle valve 24, respectively. This way all the experimental conditions were reached by using only CO_2 as supply so the mixture of carbon dioxide/methanol was not wasted in the starting up of the system. When all the values of temperature and flow rate were constant and equal to the intended, the supply line was switched to the mixture 8, using the line valves 6 and 9. When this change in the supply line was made there was a little pressure variation inside the reactor that was corrected by setting again the pressure controller 12 or the pressure regulator 17.

When there was seen alcohol condensation at the refrigeration bath, 26, the flow rate is checked in the flow meter 27, and if there is any variation, it is corrected by using the needle valve 24 to maintain the intended value. Then when the mixture of CO2/Methanol is passing through the reactor, the oil pump is switched on and set to the intended flow rate, and the line valve 3 is opened. At this point everything is ready for the reaction to take place, and only a few minutes later the effluent starts to be seen inside the collecting vase 25, in the heated bath. To make sure the system is in steady state the operation was carried out during at least 10 times the residence time inside the reactor. Only after this determined time interval, the collecting vase was switched to a clean one, and the sample was collected. When there was about 25 mL of sample collected the vase was removed the sample transferred to a separating funnel to future analysis. Then the oil pump 2 as turned off, the feed line close by valve 3, and the gas feed line changed again to carbon dioxide. The system was depressurized by shutting down the pump (closing the supply air pressure) and was left to lose pressure gradually to

remove all the remaining products in the reactor. The temperature controllers were also turned off to gradually cool all the system.

3.3 Analytical Technique

After evaporating the unreacted methanol, the samples were left, preferably overnight, in a separating funnel to let the glycerol layer separate from the esters layer. Then a sample of the upper layer was collected and stored to future analysis. In Figure 13 there is a picture taken to some samples were both layers of esters and glycerin are clearly separated.

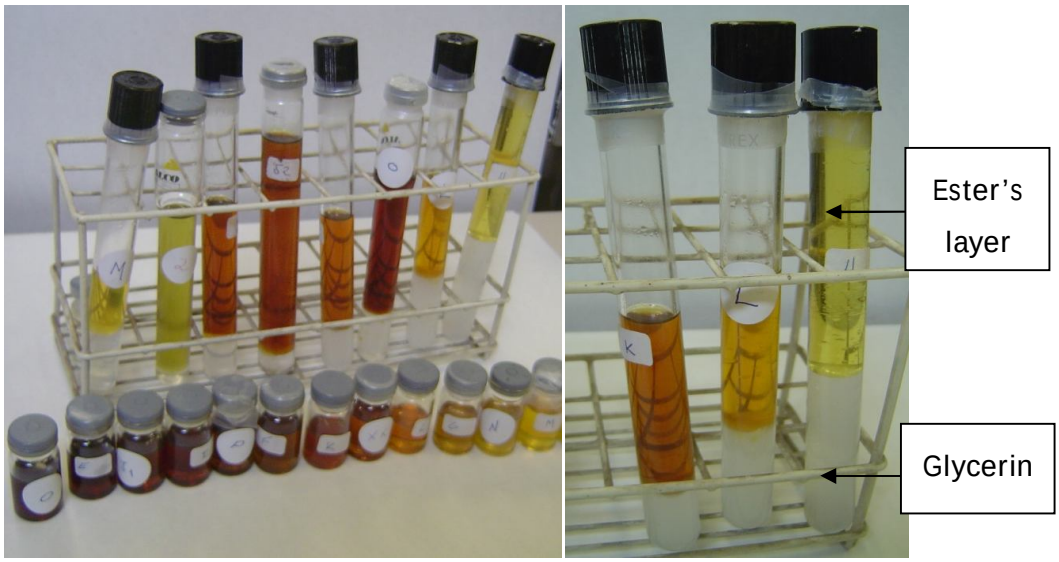

Figure 13: Samples of the reaction mixture collected.

The reaction samples were analyzed by gas chromatography, a Shimadzu CG-2010 chromatograph shown in Figure 14. Each sample produced was analyzed by two different methods, one for the quantification of fatty acid methyl esters (FAMEs) and other to determine the quantity of triglycerides, dyglycerides, monoglycerides and glycerin present in each sample.

Figure 14: View of the gas chromatograph Shimatzu 2010 with FID detector

3.3.1 Determination of the fatty acid methyl esters (FAME) content

For the determination of the FAMEs percentage in each sample it was used a variable flow split injector (split/splitless), a capillary column and for detection a flame ionization detector (FID). The capillary column employed was a Teknokroma SupraWax-280 with an internal diameter of 0.32 mm, a length of 30 m, a film thickness of 0.25 µm and a stationary phase of poliethyleneglycol (PEG). A standard mixture of methyl esters was used for the qualitative analyses and a methyl heptadecanoate (both were purchased from Sigma Aldrich, Barcelona, Spain) was used as the internal standard for the quantitative determination of FAMEs. The analyses were conducted under the EN 14103:2003 European standard method. [17]

The column temperature was programmed from 120 ºC, holding 1 min, ramp at 10 ºC to 170 ºC, 2ºC/ min to 190 ºC and then 200 ºC at 25 ºC/min and remaining for 11 min. Total run time for this method was 28 min. In appendix it is shown a chromatogram of an experimental sample produced. The determination was the fatty acid methyl esters content was done accordingly to the referred European standard method and can be found in the same appendix to this work.

3.3.2 Determination of free and total glycerol and mono-,di-, triglyceride contents

For the determination of the free and total glycerol, mono di and triglycerides present in the produced samples was used an on-column injector (Shimatzu) a capillary column and a flame ionization detector (FID). The capillary column used was a Teknokroma TRB-Biodiesel fused silica column with an internal diameter of 0.32 mm and 10 m of length. It also had a 0.53 mm internal diameter and 2m long pre-column attached with an inox connector. The film thickness of the column is 0.10 µm and its maximum operating temperature is 400ºC.

The analyses were conducted under the EN 14105:2003 European Standard Method. The principle is the transformation of the glycerol, mono,di and triglycerides into more volatile silylated derivatives in presence of pyridine and of N-methyl-N-trimethylsilyltrifluoroacetamide (MSTFA).

After the calibration procedure, the quantification is carried out in the presence of two internal standards: 1,2,4-butanetriol intended for the determination of the free glycerol; and 1,2,3-tricaproylglycerol (tricaprin) intended for the determination of the glycerides (mono-, di- and tri-). The calibrations curves, the repeatability tests and the method for calculating each glyceride content can be found in appendix to this work as well a chromatogram of one of the biodiesel samples produced.

The column temperature was 50ºC, hold for 1 minute, programmed at 15ºC/min up to 180ºC, programmed at 7ºC/min up to 230ºC, programmed at 10ºC/min up to 370ºC, and hold the final temperature for 5 minutes. The detector temperature was set to 380ºC , the carrier gas was helium, and the volume injected was 1µL.

4 Supercritical properties of the mixture CO_2-Methanol-Sunflower oil

Some previous studies in the modeling of phase equilibria have been made in the chemical engineering department of ESTEIB by the investigation group where this work has been carried out, and their results were compared with some experimental published data [18] [19].

To produce biodiesel in supercritical conditions, a previous study has to be done in order to determine in which conditions the reactor should be operated. The transesterification rate is low at subcritical (multiphase) conditions but significantly accelerated at supercritical (single phase) conditions. A portion of this acceleration is due to temperature effects, but a portion is also due to the presence of a single supercritical phase at supercritical conditions. Therefore, the phase behavior of the mixture in the system is an important consideration in biodiesel production. Large excess amounts of alcohol have been used in previous supercritical transesterification researches because this practice reduces the critical temperature of the mixture.

The critical properties of triglyceride-alcohol mixtures have not been a topic of much research, so the precise amount of alcohol needed to achieve supercritical conditions at a given temperature is not readily available. In this work a preliminary phase behavior study of methanol/CO_2 –sunflower oil was done, to assess the minimum operating conditions of pressure and temperature that the reactor should be operated to achieve the supercritical single phase condition. In this project it was decided to use CO_2 co-solvent as their use can decrease the mixture critical point and allow the reaction to be carried out under milder conditions, enhancing the mutual solubility of the oil-alcohol mixture [20] [16], and reducing the transport limitations and increasing reaction rates. [21] The Peng-Robinson (Peng and Robinson 1976) equation of state was used to estimate the critical point of the mixture for a determined molar composition of a mixture of 1% sunflower oil:99 % of methanol/CO_2 (25% methanol:75%CO_2).

4.1 Thermodynamic Modeling

Sunflower oil is composed mainly of triolein and trilionolein, with minor contents of tripalmitin, tristearin and other triglycerides. However, to simplify the problem, it is convenient to represent the complex composition of sunflower oil with a pseudo component. In this case, the selected pseudo component was triolein and not trilinolein, since it is the

components for which more thermodynamic data is available in the literature [22]. The critical constant of the pure components are needed for the calculation of *a(T)* and *b(T)*, but these constants are not available for compounds such as fats, since they are chemically unstable and decompose at high temperatures. The critical properties and other parameters of the pure components are listed in Table 3.

Table 3: Critical properties and substance parameters in equation of state

Components	Molecular weight ($kg.kmol^{-1}$)	Critical Temperature Tc (K)	Critical Pressure Pc (bar)	Acentric factor ω
Methanol	32	512.6	80.1	0.5659
CO2	44	304.2	73.8	0.225
Triolein	884	977.8	3.34	1.9780

To simplify the problem it was decided that the thermodynamic analysis would be done considering a binary system, by treating the mixture methanol/CO_2 as one component and the sunflower oil another component. Although is a rough consideration, the result should give an idea of the minimal operating conditions of the reactor.

The *Peng-Robinson* equation of state (PR-EOS) was used to correlate the experimental data. The equation can be expressed as following:

$$P = \frac{RT}{V-b} - \frac{a(T)}{V^2 + 2bV - b^2} \tag{4.1}$$

For a pure component i, the parameters a_i and b_i in the PR-EOS are function of the critical temperature, critical pressure and acentric factor of the component.

To model the molecular interactions between components i and j, the binary interaction parameters ($k_{a,ij}$, $k_{b,ij}$) are introduced through the mixing rules as follows [23].

$$a = \sum\sum x_i x_j \sqrt{a_i a_j}\left(1 - k_{a,ij}\right) \tag{4.2}$$

$$b = \sum\sum x_i x_j \frac{b_i + b_j}{2}\left(1 - k_{b,ij}\right) \tag{4.3}$$

where P is the pressure, R is the gas constant, T is the temperature, and V is the molar volume. The parameters a and b are the energy and size parameters, respectively. The subscript c denotes the critical properties. The experimental data of the critical properties and the acentric factor (ω) for alcohols and sunflower oil are available from the literatures [22][24], and

can be seen in appendix of this work (Determination of the critical properties of Methanol/CO_2 mixture).

The experimental information available in the literature on high-pressure phase equilibrium of reactive mixtures is very scarce, which made difficult to determine the model parameters. An additional problem was faced with the vegetable oil because its pure component properties such as vapor pressure and critical properties are experimentally unattainable due to their low volatility and thermo liability. Thus, it was necessary to make a rough theoretical estimation of its critical properties according to the Chueh–Prausnitz approximation [(24)]. The estimated values are presented in Table 4. All the calculations of the thermodynamic parameters for each composition of the mixture can be found in appendix.

Table 4: Estimation of the critical properties of the Methanol/CO_2 mixture by the Chueh-Prausnitz approximation

Molar composition of Methanol/CO_2 (percentage of methanol)	Critical Pressure P_c (bar)	Critical Temperature T_c (K)	Acentric factor, ω
0.05	90.15	320.78	0.24
0.10	103.34	336.55	0.25
0.15	113.88	351.55	0.27
0.20	122.17	365.79	0.28
0.25	128.50	379.32	0.29
0.30	133.11	392.16	0.31

As can be observed from Table 4 the introduction of the carbon dioxide co-solvent decreases the critical properties of the mixture. As the quantity of methanol increases in the binary mixture (decrease in the percentage of CO_2) the critical pressure and temperature increase. The molar composition chosen to work with was a mixture of 25% of methanol.

With the critical properties defined for the methanol/CO_2 defined, this mixture was treated as one component, and the sunflower oil (triolein) was treated as another.

The determination of the critical temperature and pressure of this mixture was done by using the phase equilibrium program called PE-2000. This program was developed by Professor's Brunner research group at the Technical University of Hamburg [(25)]. PE-2000 is built in order to obtain an efficient tool to correlate phase equilibria, especially those at high pressure. This program offers more than 40 equations of state, and as was mentioned the one chosen was the Pen-Robinson equation of state.

So the input in the PE-2000 program was the pure component critical data from both components, being one of them the Methanol/CO2 other triolein, presented in Table 3.

The program's outputs were the vapor/liquid constants, k_1 and k_2, by varying the pressure value, maintaining a constant temperature. There was chosen three values of temperature, 150, 180 and 205 ºC.

The binary vapor–liquid equilibrium (VLE) diagrams for sunflower oil in CO2 + alcohols are shown in terms of the VLE constants as a function of pressure at constant temperature in Figure 15.

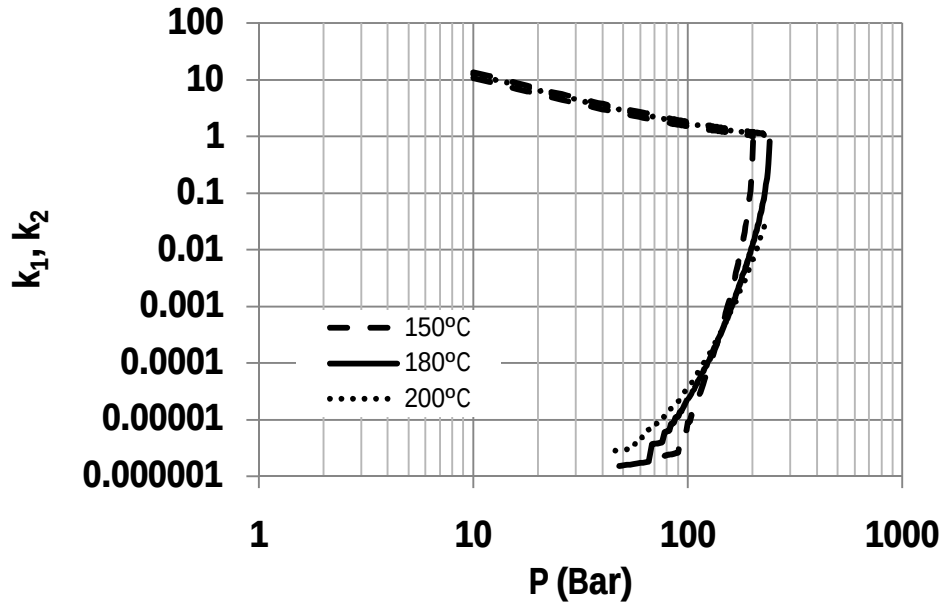

Figure 15: Binary vapor liquid equilibrium diagram for the mixture CO2/methanol and sunflower oil

The determination of the critical point was calculated for the system CO2+methanol–sunflower oil, estimating the *Ki* values from the fugacity coefficients calculated with the PR-EOS [(26)(27)]. The calculations were performed with the PE 2000 [(25)] in terms of the convergence pressure[(28)]. The critical pressures for each constant temperature were determined by both the convergence of vapor and liquid equilibrium lines and are presented in the following table.

Table 5. Determined critical pressures for each operating temperature

Mixture molar composition	Temperature (ºC)	Pressure (bar)
Methanol/CO_2 (99%) + Triolein (1%)	150	200
	180	240
	205	245

To ensure the supercritical single phase condition the pressure was help above the determined necessary value, and was chosen constant and equal to 250 bar for each operating temperature.

5 Transesterification Reaction

5.1 Theoretical

The continuous flow experimental setup was already described in the previous chapter. In the present chapter experiments of transesterification of sunflower oil with a solid catalyst are presented.

Sulfonic resins are part of a group of acid catalysts that are classified according to its polymer backbone, namely polystyrene (for example Amberlyst® resins) or perfluorinated alkanes (Nafion® resins for instance)[29]. These acid resins have inherently low surface areas unless a solvent is used to swell the polymer and thus exposing additional internal active sites for reaction. Because in heterogeneous catalysis high surface areas are of the most interest, increased surface area of catalyst can be achieved by dispersing the polymer on high surface area materials, such as inert oxide materials.

The catalyst employed in this work is one of these materials. It is a silica-supported sulfonic acid polymer, Nafion® SAC-13 shown in a picture taken presented in Figure 16.

Figure 16. Picture of the Nafion SAC-13 acid catalyst used.

It's a highly acidic Nafion® silica nanocomposite that contains 13 wt% Nafion, which is a colpolymer of tetrafluoroethylene and perfluoro-2(fluorosulfonylethoxy)propyl vinyl ether. The small (5-30 nm) Nafion® resins particles are entrapped within the porous silica matrix. A detailed list of its characteristics is shown in appendix .

The choice of this catalyst was based on numerous aspects. Because one of the main objectives of this work was to perform the transesterification reaction under supercritical conditions and with a heterogeneous catalyst, it was necessary a solid catalyst that could be used at relatively high temperatures. Information by the manufacturer stated that Nafion® SAC-13 could be used in temperatures up to 220ºC. This temperature ensured that, for the

system in study, there would be a large range of temperatures in which the reaction could take place. For security reasons the maximum temperature that the reactor was operated was set to 205ºC to avoid any damage to the catalyst. Another reason was the possibility to use this catalyst without any kind of pre-treatment, such as swelling. As stated above, these kind of acid resins often need to be treated with a solvent to swell the polymer to increase its surface area. Because Nafion® SAC-13 is supported in a porous silica matrix, this was no longer necessary. It was also reported [30] that this catalyst showed no dependency of catalytic activity on solvent pre-contact and also more efficient use of the resin acid sites (i.e, unrestricted accessibility of the reacting molecules to the active sites). In other publications was also reported that SAC-13 catalysts were reused several times in a fixed bed recirculating reactor, over long runs of about 48 hours, without significant loss of activity showing that this catalyst can be used in this reaction in a continuous way without suffering deactivation [31]. All of these factors made Nafion® SAC-13 the choice for the heterogeneous catalysis of vegetable oil.

The amount of catalyst to use was base on a practical basis. When the experimental setup was ready, several runs were made starting with only 1 g of catalyst. The results showed very low FAMEs yield (1-3%), so it was decided to use the amount correspondent to the reactor capacity. For the dimensions of this particular equipment was nine grams of Nafion SAC-13.

5.1.1 Chemistry of the reaction

The reaction scheme for the transesterification reaction of sunflower oil is presented in Figure 17.

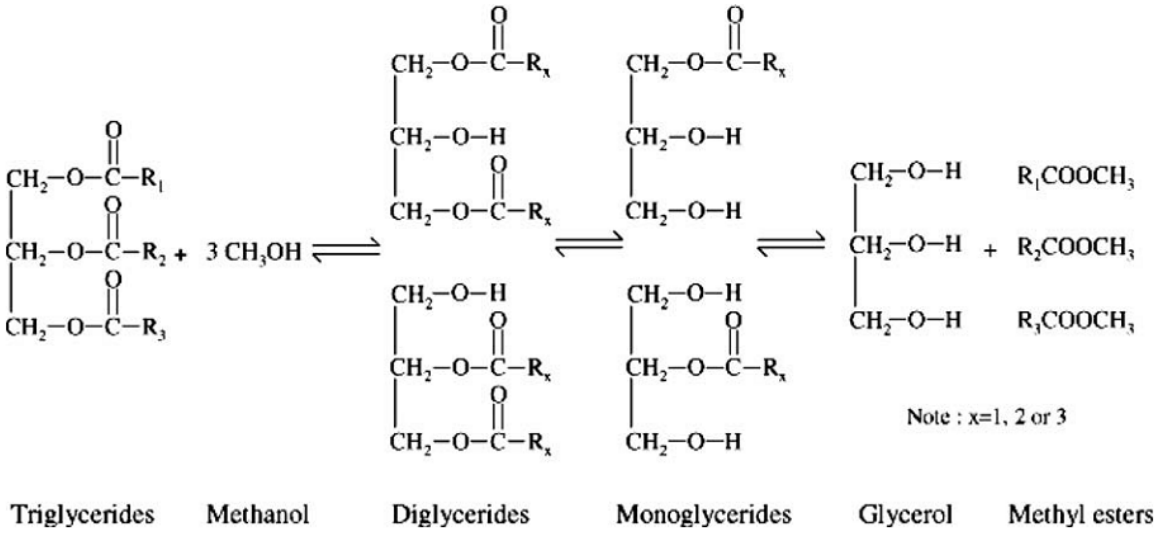

Figure 17: Triglyceride transesterification reaction scheme

The stoichometry of reaction requires three mol of methanol and one mol of triglyceride to produce three mol of fatty acid methyl esters (FAME) and one mol of glycerol.

This reaction consists on three consecutive reversible reactions, where in each one, one mol of methyl ester is liberated and mono and diglycerides are intermediate products [(1)(3)(7)(32)]. Figure 17 shows a scheme of these reactions where k1, k3 and k5 are the forward rate constants and k2, k4 and k6 are the reverse rate constants.

The reaction reactives -sunflower oil and methanol- are not miscible at ambient temperature and pressure; for this reason in a typical transesterification reaction the reaction system consists of two layers at the initial stage. In this sense the mass transfer controls the kinetics, until there is formation of methyl esters in the system that acts as a co-solvent because they are miscible in vegetable oil and also in methanol. However, operating the system in supercritical conditions the system becomes a single homogeneous phase, which will accelerate the reaction because there is no interphase mass transfer to limit the reaction rate[(33)]. This fact is discussed with more detailed in chapter 6.2.

5.2 Fixed bed reactor

The reactor employed in the transesterification reaction was a titanium reactor (Eurotechnica, HPA 500), shown in Figure 18, and was operated as a fixed bed reactor. It is 152 mm of length and 15.5 mm of internal diameter.

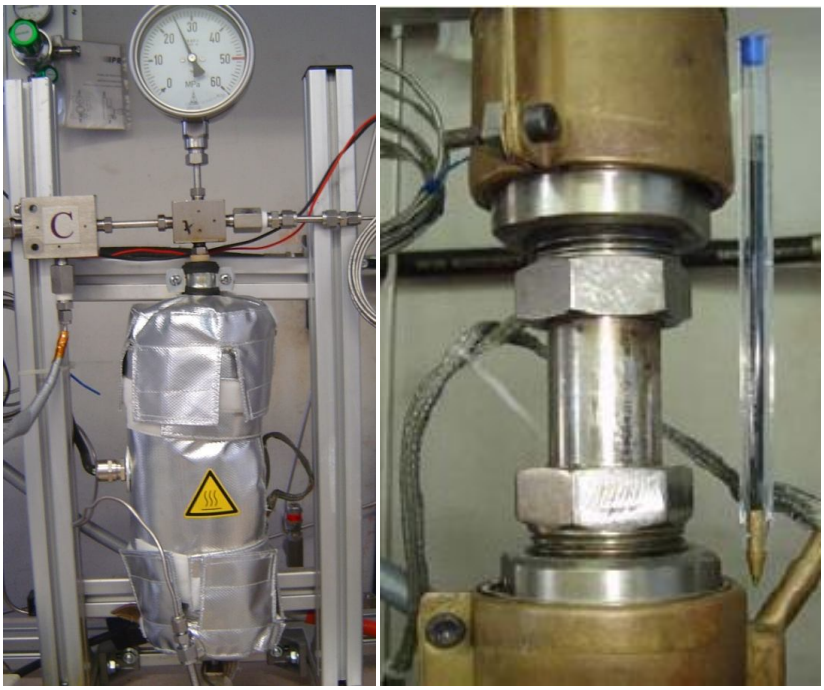

Figure 18 : Titanium fixed bed reactor (Eurotechnica, HPA 500).

The conceptual assumptions made for the flow model are mathematically described below and will be validated in the results section of this chapter.

There are several models with different degree of complexity that can be applied to the modeling of fixed bed reactors. This matter has been well studied and reviewed by Froment (1970) and Froment and Bischoff (1990)[34]. These authors classified the models of fixed bed reactor into two major categories: Pseudo-homogeneous and heterogeneous models, where the first group does not account for interfacial and intraparticle gradients, contrary to the second group. Pseudo homogeneous models do not account explicitly for the presence of catalyst, in contrast with heterogeneous models, which lead to separate conservation equations for fluid and catalyst [34].

In this work there will be used an one dimensional heterogeneous model, that considers only transport by plug flow, but distinguishes between conditions in the fluid phase and on the solid.

The steady state equations are, for a single reaction carried out in a cylindrical tube and with the restrictions already mentioned for the basic case:

Fluid

$$-u_s \frac{dC}{dz} = k_g a_v (C - C_s^s) \tag{5.1}$$

$$u_s \rho_B C_p \frac{dT}{dz} = h_f a_v (T_s^s - T) - 4\frac{U}{d_t}(T - T_r) \tag{5.2}$$

Solid

$$\rho_B r_A = k_g a_v (C - C_s^s) \tag{5.3}$$

$$(-\Delta H)\rho_B r_A = h_f a_v (T_s^s - T) \tag{5.4}$$

With boundary conditions:

$$C = C_0 \qquad at\ z = 0 \tag{5.5}$$

$$T = T_0 \tag{5.6}$$

Based on the equations from (5.1) to (5.6) there can be written the mass balance equations used for the determination of the concentrations of the reactive in terms of space time inside the reactor:

$$-(r_T)_{obs} = \frac{dF_T}{dW_{cat}} = \frac{C_{T,e}}{\rho_B}\frac{dx_T}{d\tau} \tag{5.7}$$

In this work the experiments were conducted under isothermal conditions, so the heat transfer rate equations (5.2),(5.4) were not included in the treatment of the problem

Table 6: Names and units of the terms used in equation (5.7)

Name	Equation Term	Units
Observed reaction rate of triglyceride disappearing by reaction	$-(r_T)_{obs}$	$mol.kg_{cat}{}^{-1}.min^{-1}$
Derivative of conversion of triglyceride in order to space time	$\frac{dx_T}{d\tau}$	$kg_{fluid}.kg_{cat}.min^{-1}$
Initial triglyceride concentration	$C_{T,e}$	$mol.m^3_{fluid}$
Bulk density	ρ_B	$kg_{fluid}.m^3_{fluid}$

6 Results

As the main goal is to produce biodiesel in continuous flow, various experiments were performed in the previous described installation. These experiments followed the procedure described in the chapter 3.3. In the following sections the influence of the operating conditions in the installation is studied, and then the results obtained are interpreted to give some insight in the transesterification reaction.

6.1 Influence of the operating conditions – Response Surface methodology

To assess the influence of the operating conditions in the production of biodiesel, the analysis of the methyl esters produced by transesterification of sunflower oil was carried out using a central composite design of experiments. A two variable design was applied, and the ester content in the biodiesel samples was selected to be the response variable.

The variables investigated were the temperature inside the reactor and the space time. The selection of levels for each variable was based on the experimental limitations of the operating conditions. The temperature was varied between 150 and 205 ºC. The lower limit was set by the supercritical single phase condition, at 250 bar, and the upper limit by the maximum operating temperature of the catalyst employed. The space time was varied between 0.5 and 4 minutes. These limits were due to the flow rate employed, which was conditioned by the pump used and the expansion valve placed after the reactor (see chapter 3.3 – System operation).

The analysis was conducted using coded variables, where the meaning of each coded variable is explained in Table 7.

Table 7: Coded variables used in the regression

Coded Variable	Variable
$Y_{FAMEs\,\%}$	Fatty acid methyl ester content
X_T	Coded variable for temperature
X_τ	Coded variable for space time

Once these levels were selected the central composite design of experiments was applied. The experimental conditions studied in this work are presented in appendix C – Experimental conditions studied: central composite design.

Twelve experiments were performed, varying the temperature inside the reactor and the mixture inlet flow rate, and thus the space time inside the reactor. The oil flow rate was calculated in each run so the methanol/oil molar ratio was kept constant throughout the experiments, and equal to 25. The pressure and catalyst amount were also kept constant at 250 bar and nine grams respectively. In Table 8 are presented the operating conditions in each run and the content (mass percentage) of each sample in terms of fatty acid methyl esters.

Table 8: Operating conditions and FAME's content in each run

Run	Temperature *ºC*	Pressure *bar*	Catalyst mass *g*	Mixture Flow rate *mL.min^{-1}*	Oil flowrate *mL.min^{-1}*	Methanol /oil molar ratio	Residence time *min*	FAMEs %
1	150	250	9	18,0	0,788	25	0.5	7,9
2				9,40	0,411		2.1	15,1
3				5,20	0,226		3.9	37,3
4				35,7	1,56		1.0	10,1
5	180	250	9	7,96	0,256	25	3.9	70,0
6				12,8	0,411		2.1	74,5
7				25,9	0,834		1.0	68,2
8				48,7	1,56		0.5	32,5
9	205	250	9	28,7	0,834	25	1.0	78,1
10				14,1	0,411		2.1	81,6
11				8,78	0,256		3.9	79,2
12				53,7	1,56		0.5	64,1

The content of each sample in terms of fatty acid methyl esters was determined by gas chromatography, following the procedure described in chapter in appendix to this work. The values of FAME's percentage were plotted in function of temperature and space time and can be seen in Figure 19.

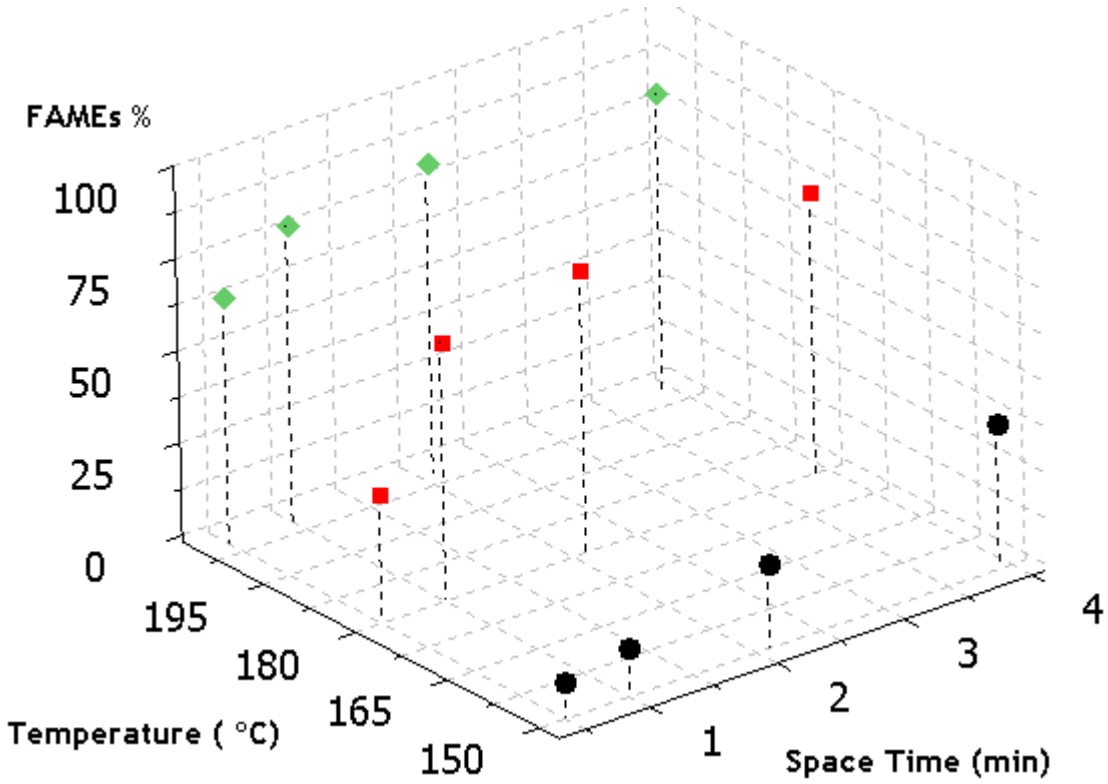

Figure 19: Three-dimensional scatter plot of the response in FAMES % in each run performed. Pressure = 250 bar, catalyst mass = 9 g, methanol/oil molar ratio = 25.

The multivariable analysis of data is a powerful statistical technique used for studying the effect of several factors and their interactions over one or more response variables in a process.[35]

In this work, response surface methodology, which has been used for biodiesel production optimization [36] , was performed on experimental data and, as a result, a lineal regression quadratic model was obtained, as shown in the following equation, for the transesterification of vegetable oil with methanol.

$$Y_{FAMEs\,\%} = 70.295 + 27.639X_T + 13.167X_\tau - 12.966X_T^2 - 11.867X_\tau^2 - 4.343X_\tau X_T \qquad (6.1)$$

The values and p-value associated with each coefficient of this model can be seen in Table 9. According to Montgomery [35] the p-value represents the minimum significance level of a group of data or variable in a statistical hypothesis test.

Table 9: Coefficients of the lineal regression quadratic model and their respective p-value associated

Coefficient	Value	p-value
b_0	70.295	0.000
b_{X_T}	27.639	0.000
b_{X_τ}	13.167	0.0050
$b_{X_T{}^2}$	-12.966	0.0370
$b_{X_\tau{}^2}$	-11.867	0.0610
$b_{X_T X_\tau}$	-4.343	0.299

According to the p-values presented the model demonstrates a good adjustment with experimental data and is also statistically significant. The coefficient of determination R^2 approaches one (0.94) indicating that the regression proposed has a good prediction capacity, for the system at hand.

Figure 20 plots the experimental versus correlated values for biodiesel production using sunflower oil. The plot reveals that there is no tendency in the linear regression fit, which indicates that the model explains well the experimental range studied.

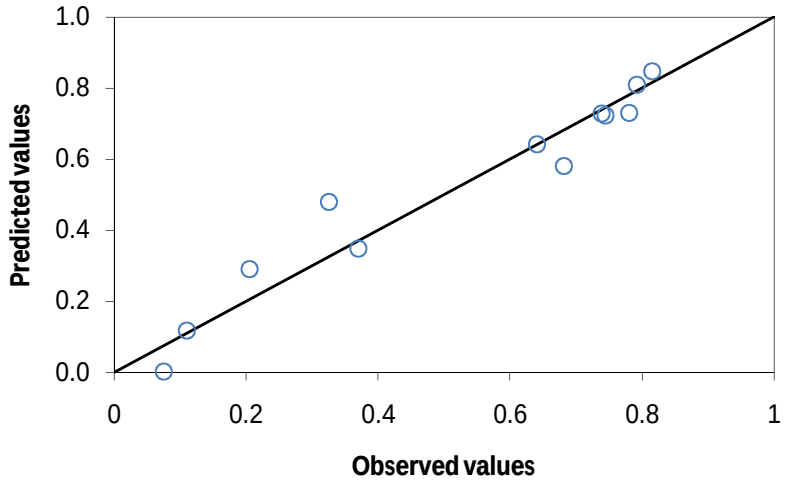

Figure 20. Experimental observed values and predicted values from the lineal regression

According to the p-values obtained from the statistical analysis, and in the experimental range studied, the temperature inside the reactor is the most important factor in the production of biodiesel in the experimental setup built (lowest p-value).

Figure 21 helps identify the types of interaction between the variables that affect the reaction. It represents the response surface for the ester content (in mass percentage) for a constant methanol/oil molar ratio, pressure and catalyst amount. The maximum ester percentage is achieved at the maximum temperature, 205ºC, but not for the maximum value of

space time. As will be discussed later there was a decrease in the FAMES percentage for 180 and 205ºC, at low flow rates, this is low values of space time. This led the model to predict a maximum value of conversion of triglycerides at a space time of 2.7 minutes at 205ºC, of 86.6%.

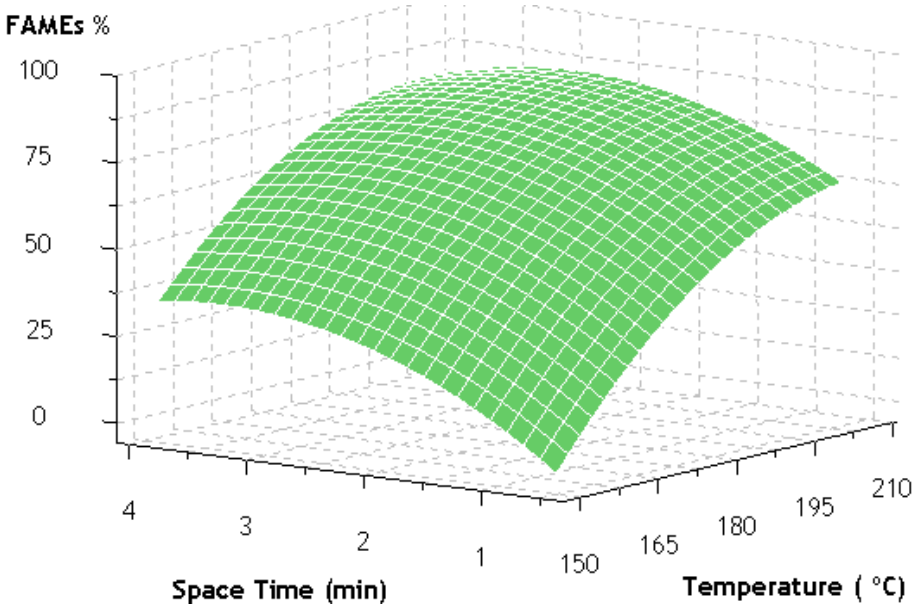

Figure 21: Response surface of ester percentage verus space time and temperature. Pressure = 250 bar, catalyst mass = 9 g, methanol/oil molar ratio = 25.

6.2 Determination of the Reaction Rates

The analysis of the fatty acid methyl esters, triglycerides, diglycerides, monoglycerides and glycerol were conducted in each sample using the chromatographic methods described in a previous chapter. The content of FAMEs versus space time in Figure 22 is plotted, for each of the operated temperatures.

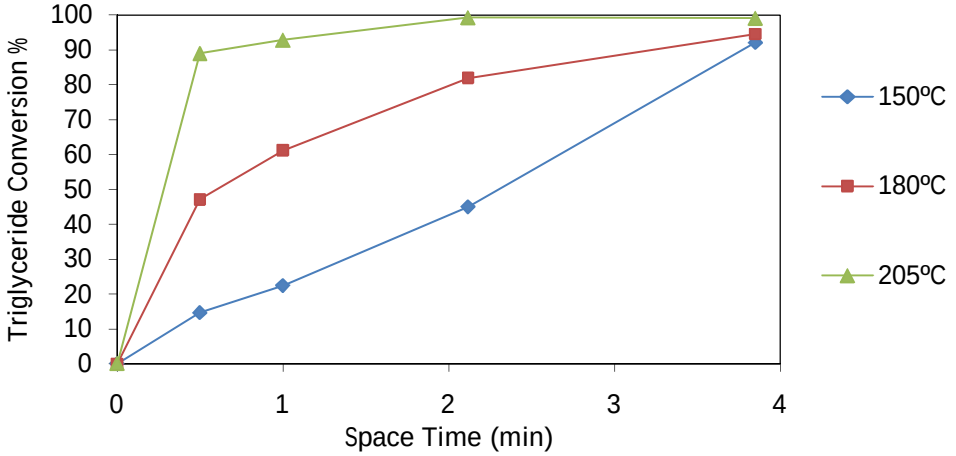

Figure 22: Effect of the temperature and space time in the content of fatty acid methyl esters. Pressure = 250 bar, catalyst mass = 9 g, methanol/oil molar ratio = 25.

From the data represented it can be seen that the conversion of triglycerides increases with temperature and with space time. In the case of the high temperatures, 180ºC and 205ºC, the production of methyl esters increase very rapidly, and at 205ºC there is a production of 80% of FAMES at a mixture space time of only one minute. For lower flow rates that result in space time higher than one minute, at 180 and 205 ºC, the equilibrium is apparently reached, as the content of esters does not change significantly.

At 150ºC and for the experimental conditions used the FAMEs content doesn't reach a constant value, and so the equilibrium is not reached. More experiments at this temperature will have to be performed to evaluate the kinetics at this temperature, particularly by changing the inlet flow rate to obtain more experimental points with higher values of space time. There is clearly an important difference between in the reaction rate from 150 ºC to 180 ºC, which is an indicator that the reaction rate constants are highly dependent on the value of temperature.

In Figure 23 is shown the influence of the operated flow rate in the reactor in the conversion of triglycerides, for each operated temperature. As can be seen, for any space time in the reactor, the highest conversions of triglyceride are obtained using the highest temperature, 205ºC.

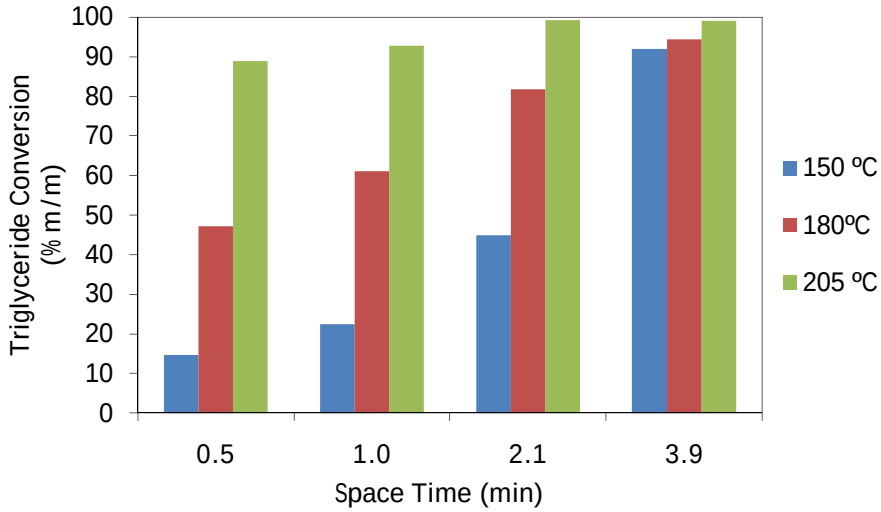

Figure 23: Effect of the temperature and space time in the triglyceride conversion. Pressure = 250 bar, catalyst mass = 9 g, methanol/oil molar ratio = 25.

The difference in the conversion between the three temperatures is more evident for higher flow rates that result in low values of space time. For lower flow rates the conversion of triglyceride tends to be the same, and approached 100% with little difference between 150, 180 and 250ºC. From this it can be drawn that the influence of temperature is more important at higher flow rates, this is low space time values when the reaction is in the beginning and the

corresponding reaction rate is at its maximum. Because the temperature has an exponential influence in the reaction rate constants, at the beginning of the reaction when the reaction rate is maximal, because there are no formed products, this influence is more evident, and thus the difference in conversion is greater between temperatures at low space times when compared to the difference verified at higher space times, as it is shown in Figure 23 .

Making use of the mass balance expressed in equation (5.7), and from the slopes of the curves represented in Figure 22 the observed reaction rates can be calculated. For this, in each run has to be calculated the bulk density, a property that varies with pressure and temperature [(23)]. For this calculations was used the Peng-Robinson equation, which can be seen with more detail in appendix to this work. From that picture is possible to see that the bulk density is constant for each operating temperature. As expected the increase in temperature, at constant pressure, decreases the density of the mixture inside the reactor. For the operating conditions used the bulk density varies between 300 and 450 $kg.m^{-3}$.

In Table 10 are presented the values of the observed reaction rate for each run. For each temperature the reaction rate has its maximum for high values of flow rate, this is low values of space time. This was to be expected as in the beginning of the reaction the concentration of reactants is maximum and lowest for the products.

Table 10: Observed reaction rate in each experiment

Run	Temperature	Space Time	Conversion of Triglycerides	Observed Reaction Rate
	ºC	*min*		*mol.kg $_{cat}^{-1}$.min^{-1}*
1	150	0,5	0.146	0.0874
2		1,0	0.224	0.0466
3		2,1	0.450	0.0605
4		3,9	0.921	0.0812
5	180	0,5	0.471	0.2850
6		1,0	0.611	0.0848
7		2,1	0.818	0.0561
8		3,9	0.945	0.0220
9	205	0,5	0.889	0.5393
10		1,0	0.927	0.0232
11		2,1	0.993	0.0177
12		3,9	0.990	-0.0004

As the reaction progresses in time (in this case with space time) equilibrium is approached and the reaction rates start to decrease. When equilibrium is reached there is expected that the reaction rate of disappearance of triglycerides is zero. As can be seen from

Table 10 in run 8 and 9 this value is close to zero. The negative signal does not have any meaning, as at the operated temperatures there shouldn't be any thermal decomposition. Kusdiana and Saka [37] reported that the decomposition reaction took place at 400ºC, value that is much higher than the maximum operated temperature in this work, 205 ºC. There is also the possibility that the negative values of reaction rate could mean that there are some unknown side reaction for this system. However, in this work, there aren't sufficient experimental data to prove this claim. At 150ºC the reaction rate does not decrease until a space time of 4 minutes, as the reaction is still far from the equilibrium as can be seen in Figure 22.

In Figure 24 the observed reaction rate is plotted with temperature and space time. Here the progress of the reaction can be evaluated. At 150ºC the reaction rate is constant for any of the values of space time used in this work, which indicated that, at this temperature, the reaction does not reach the equilibrium as stated before. At 180ºC there is clearly a decrease of the reaction rate from the 0,5 and 1 minutes to 2 and 4 minutes of space time. Equilibrium is reached as for these values of space time the observed reaction rate is zero. This is even more evident at 205ºC because the data points from 0,5 and 1 minutes are very different, indicating that the reaction rate is much higher at this temperature, reaching equilibrium in almost one minute of spate time inside the reactor. These observations corroborate those drawn from Figure 22, where the conversion of triglyceride is plotted, for each temperature, against space time.

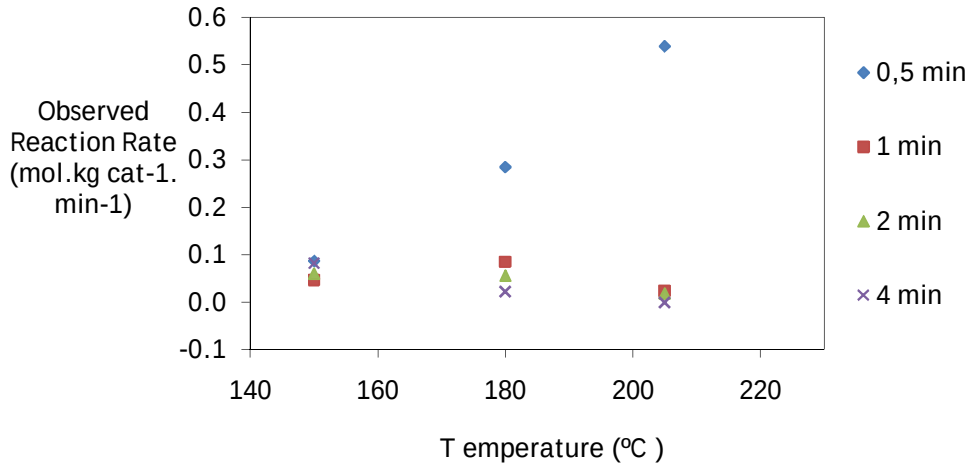

Figure 24: Influence of temperature and space time in the observed reaction rate

6.2.1 Kinetic modeling

Once determined the observed reaction rate, the reaction rates constants can be calculated, by writing the reaction rate equation. As was stated above, the transesterification reaction is a series reaction. Each step is reversible and produces one mol of fatty acid methyl esters.

In this work the reaction rates constants are determined by two different ways: considering the reaction as irreversible and in one single step, and other considering the reaction as a series of three consecutive reversible reactions. Each method is described in the following sections.

Buy first, for the kinetic study some assumptions have to be made:

i. As the sunflower oil is refined, the proportion of free fatty acids is negligible, and then the free fatty acid acid neutralization was not significant.

ii. The mass transfer resistance from fluid to solid is shown to be insignificant, and therefore the chemical reaction stage controls the reaction rate. This assumption is explored in detail in the following section.

6.2.1.1 Mass transfer

Transport phenomena can seriously interfere with the reaction itself, and great care should be taken to eliminate these as much as possible in kinetic investigation.[34] In this chapter the mass transfer coefficients are calculated and the unmeasured surface concentration is determined and compared to that in the bulk to assess the mass transfer resistance in the system. The mass transfer coefficient is defined in transport processes. As heat transfer, mass transfer depends on conditions of state, so as the reaction is carried out in supercritical conditions, the mass transfer coefficients are not available easily in open literature. In supercritical conditions mass transfer is studied specially in extraction problems, where some correlations have been proposed[38]. However first there are some properties of the system that have to be determined such as the viscosity and the diffusion in each experiment done.

The diffusion is transport of matter without convection or mechanically induced mixing. There are few experimental studies of binary diffusion coefficients at high pressures, and many of the data involve a trace solute. Takahashi has suggested a very simple corresponding states method which is satisfactory for the limited data base available[23]. His correlation is

$$\frac{D_{AB}P}{(D_{AB}P)^{+}} = f(Tr, Pr) \qquad (6.2)$$

where D_{AB} is the diffusion coefficient in $cm^2.s^{-1}$, and P the pressure in *bar*. *Tr* and *Pr* are the reduced temperatures and pressure respectively. The superscript + indicates that the low

pressure values are to be used. The determination of the low-pressure values was calculated by the Fuller[23] method. All of these calculations can be found with detail in Appendix.

Viscosity also had to estimated for the system at hand, and it is an important parameter as it influences mass transfer. It is well known that dissolved supercritical carbon dioxide reduces viscosity of a substance in the liquid phase, since Kuss and Golly published their results [38]. Viscosity in the saturated liquid phase decreases with increasing pressure, which corresponds to increasing amount of dissolved supercritical fluid. The following tendencies are to be expected regarding viscosity[38]:

- Viscosity o the liquid phase, saturated with the supercritical compound, decreases rapidly with pressure;
- Liquid phase viscosity decreases with temperature;
- Decrease of liquid phase viscosity is higher at lower temperatures.

So in sum, viscosity of the mixture depends on the viscosity of the solvent and the concentration of low volatile compound. For the calculation of saturated phases, the Grunberg[38] equation was employed, which for a binary mixture:

$$\eta_m = \eta_1^{X1}\eta_2^{X2}\exp\left(G_{12}x_1x_2\right) \qquad (6.3)$$

Where

η_m is the viscosity of the mixture;

η_1 , η_1 is the viscosity of pure component 1 and 2 at system temperature;

X_1, X_2 are the concentration components 1 and 2 (mole or mass fraction);

G_{12} is the interaction coefficient

The calculations of the viscosity values for each run can be seen in Appendix . In Table 11 there are presented the determined values of diffusion and viscosity for each operating temperature.

Table 11: Determined values of viscosity and diffusion coefficients

Run	Temperature ^oC	Pressure bar	Viscosity $g.cm^{-1}.s^{-1}$	Diffusion coefficients $cm^2.s^{-1}$
1-4	150	250	$7.79x10^{-6}$	$2.32x10^{-6}$
5-6	180	250	$6.18x10^{-6}$	$3.01x10^{-6}$
9-12	205	250	$5.78x10^{-6}$	$3.40x10^{-6}$

As mentioned previously, the mass transfer coefficient is defined as in transport processes, and is defined between a fluid and the particles of a packed bed by some authors. The correlations used for the prediction of these coefficients are presented in the next table.

Table 12: Correlations used for the prediction of the mass transfer coefficients

Author	Correlation	Range of validity
Brunner and Zwiefelhofer (1993), [38]	$Sh = 1.5\, Re^{0.43}\, Sc^{1/3}$	5.6<Re<28.1
Wakau and Kaguei (1982), [39]	$Sh = 2 + 1.1\, Re^{0.6}\, Sc^{1/3}$	1<Re<100
Lim et al. (1990), [40]	$\frac{Sh}{(ScGr)^{1/4}} = 0.1813\left(\frac{Re^2 Sc^{1/3}}{Gr}\right)^{1/4}\left(Re^{1/2}Sc^{1/3}\right)^{3/4} + 1.2149\left[\left(\frac{Re^2 Sc^{1/3}}{Gr}\right)^{3/4} - 0.01649\right]^{1/3}$	4<Re<135
Tan et al. (1988), [41]	$Sh = 0.38 Re^{0.83}\, Sc^{1/3}$	2<Re<55 4<Sc<16

In Figure 25 are plotted the mass transfer coefficients determined and those predicted by the correlations chosen.

The mass transfer coefficients were determined using a correlation proposed by Abaroudi et al.(1999) [27] and compared to those predicted by the correlations presented in Table 12.

This correlation is proposed by these authors in supercritical conditions with carbon dioxide and a variable amount of toluene as a co-solvent.

$$Sh = \alpha Re^{0.8} Sc^{0.33}, \text{with } 0.295 < \alpha < 0.589 \qquad (6.4)$$

Given the scarce data available in this area of study, this correlation seemed the most appropriate to determine the mass transfer coefficients and to assess the resistance of mass transfer from fluid to solid in the system.

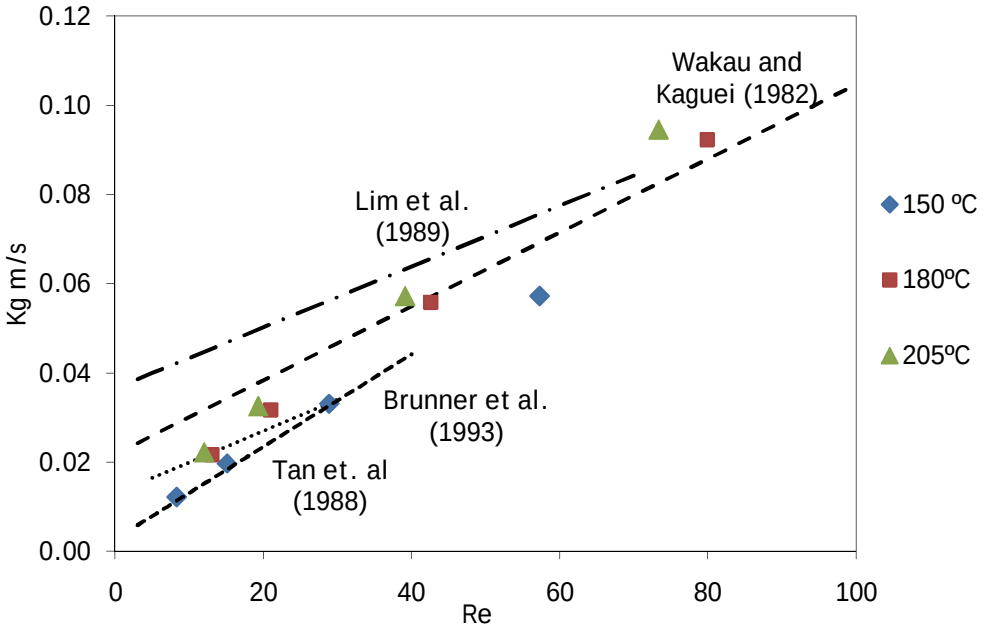

Figure 25: Comparison of predicted values of solid to fluid mass coefficients determined and for some correlations

The coefficients estimated are in the close to those predicted from the correlations. Each correlation is plotted in its range of validity, and all values of the coefficients are in range of the ones predicted from the different correlations.

In theory the mass transfer coefficients are independent of temperature[34], and as can be seen from Figure 25 these values vary very little with temperature. In appendix the coefficients were grouped by space time, and plotted in function of temperature. For each group of data with the same space time inside the reactor, increasing the temperature from 180 to 205 ºC does not affect the coefficient. A little increase can be seen to the data points corresponding to higher flow rates (space time of 30 seconds).

The determined dimensionless numbers necessary to calculate the mass transfer coefficients are presented in Table 13. Each experiment has different Reynolds and Schmidt numbers as the operating conditions are different in each case. The Schmidt relates the molecular momentum transfer (defined by the viscosity of the mixture in each experiment) and the molecular mass transfer, which is defined by the diffusion effects. As both of these parameters were calculated to each temperature (see Table 11) the Schmidt number is constant in experiments done at constant temperature.

The Reynolds number relates the total momentum transfer, this is the inertial effects, and the molecular momentum effects (defined by viscosity)[42]. As the mass flow rate is constant in experiments 1,5,9 ; 2,6,10 ; 3,7,11 and 4,8,12 (that results in experiments made in constant space time) it would be to expect constant Reynolds numbers in these experiments.

This doesn't happen because, as they are done at different temperatures, and because the mixture density varies with the temperature the volumetric flow rate necessary in each experiment to achieve the same space time is different, and thus the difference in the Reynolds number for each run.

Table 13: Determination of the mass transfer coefficients for each experiment

Exp.	Temperature (ºC)	Re	Sc	Sh	Kg (m.s^{-1})	$\frac{C_{TG,bulk}-C_{TG,surface}}{C_{TG,bulk}}$ (%)
1	150	57	7.4	25	5.73x10^{-2}	0.0000061
2		29	7.4	14	3.31x10^{-2}	0.0000058
3		15	7.4	8.5	1.97x10^{-2}	0.0000080
4		8	7.4	5.2	1.22x10^{-2}	0.0000473
5	180	80	6.2	30	9.13x10^{-2}	0.0000228
6		43	6.2	18	5.53x10^{-2}	0.0000238
7		21	6.2	10	3.14x10^{-2}	0.0000346
8		13	6.2	7.1	2.15x10^{-2}	0.0000194
9	205	73	5.6	28	9.36x10^{-2}	0.0000871
10		39	5.6	17	5.66x10^{-2}	0.0000102
11		19	5.6	9.4	3.22x10^{-2}	0.0000163
12		12	5.6	6.5	2.20x10^{-2}	0.0000005

The coefficients are also presented in Table 13 and plotted in Figure 25. With these values the resistance to the mass transfer between the fluid and solid phase could be determined. Making use of the equation (5.3) the triglyceride concentration in the catalyst surface was determined and compared to that verified in the bulk. The values are presented in Table 13 in form of percentage. As can be seen from this table, the difference between the two concentrations can be safely neglected as the maximum value for this difference is 0.00009%. The concentration gradients were also determined but with the values of the mass transfer coefficients predicted by all the correlations presented in Table 13 and all led to the same conclusion that there were no mass transfer resistance between the fluid and the catalyst. The values can be seen in appendix to this work.

6.2.2 One step irreversible reaction

In this work methanol was used in excess, in 25 times regarding the molar concentration of sunflower oil. Therefore it can be considered that the forward reaction became dominant and each reaction step could be regarded as an irreversible reaction. In addition, assuming that the methanolysis of triglyceride is the controlling rate set of the overall reaction, the transesterification reaction of triglycerides can be defined as:

$$TG + 3MeOH \rightarrow 3FAME + Glycerol \quad (6.5)$$

$$-r_{TG} = \frac{dF_{TG}}{dW_{cat}} = \frac{C_{TG,e}}{\rho_B}\frac{dx_{TG}}{d\tau} = \frac{1}{\rho_B}kC_{TG} \quad (6.6)$$

Where *k* is the reaction rate constant define in min^{-1}, and $-r_{TG}$ is the reaction rate of disappearance of triglyceride in $mol.kg^{-1}.min^{-1}$.

Making use of equation (5.11) the reaction rate constants were calculated for each experience, and are presented in Table 14.

Table 14: Determined values of observed reaction rates and reaction rate constants

Experiment	Temperature	Reaction rate constants
	^oC	min^{-1}
1-4	150	0.378
5-8	180	2.683
9-12	205	26.354

As expected the maximum reaction rate constants correspond to high flow rates, or low space time values as the concentration of reactants is maximum and of products is minimum. The exception is for 150ºC as equilibrium is no reached, and for the range of flow rates studied the reaction rate does not change significantly (as can be seen from the slopes of the curve of 150ºC of Figure 22)

In Table 15 are some reported values for the reaction rate constants. These values are drawn from authors that made the same kinetic consideration of one step irreversible transesterification reaction. Because, until the date of this work, there are not reported works that combine supercritical state of the reaction mixture with a solid catalyst, the comparison has to be made between the conventional reaction done with solid catalysts and with the conventional supercritical method. As can be seen, the values determined in this work are much higher than those reported, even when compared with higher temperatures.

Table 15: Reported values of the rate constants and activation energy for the reaction

Reference	Oil type	Temperature(ºC)	Methanol/Oil molar ratio	Catalyst	Rate Constant (min-1)	Activation Energy (kJ/mol)
This work	Sunflower	150-205	25	Nafion SAC-13	0.3-26.4	128
Dj.Vujicic et al./Fuel (2010)	Sunflower Oil	120	6	CaO	0.221	101-161
M.N. Varma et al/Fuel (2009)	mustard	300	30-80	-	0.220	59
V Rathore, G Madras /Fuel (2007)	Palm	300	10-50	-	0.114	9-15
G. Madras et al/Fuel (2004)	Sunflower	300	40	-	0.058	3
Diasakou et al	Soybean	220-235	-	-	-	117-128
E.-S. Song et al	RBD palm	200-400	-	-	-	105

The combination of the supercritical state of the reaction mixture with a catalyst apparently has advantages when comes to the reaction rate.

Plotting these reaction rate constants, corresponding to the initial conditions of the reaction (space time of 30 seconds), in function of temperature, the Arrhenius plot can be defined and the activation Energy calculated from the slope of the regression. In Figure 26 is represented the Arrhenius plot for the data points corresponding to the initial conditions of the reaction, where the reaction rate is maximum.

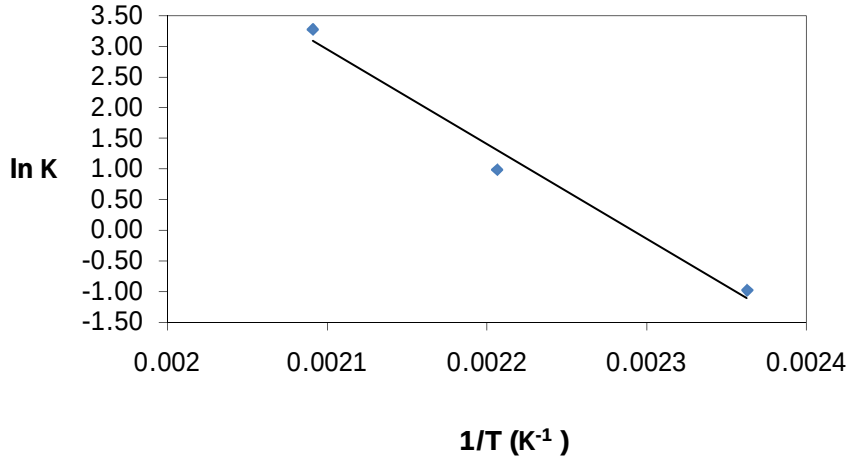

Figure 26: Arrhenius graph for data points corresponding to space time of 30 seconds

The value of the slope of the regression is -15,44 and the interception with the yy axis is 35,39. The activation energy was calculated from the slope of the regression. As can be seen

from the figure above, the data points are well fitted with a regression coefficient of 0.9829. The activation energy for this reaction was found to be 128 kj/mol or 31 cal/mol.

So far it haven't been reported works done using solid catalysts under supercritical conditions , so the values determined have to be compared to those reported in similar processes. The value determined in this work is similar to that found by Diasakou et al., and Vujicic et al.. This last author also determined the activation energy of the reaction in the diffusion regime to be 32kj/mol, indicating that value determined in this work corroborated the conclusion taken from the section 6.2.1.1 that there were no mass transfer limitations between the liquid phase and the catalyst and that the reaction is in the kinetic regime.

6.2.3 Three step reversible reaction

In the previous section the reaction was considered as a one step irreversible reaction and first order to the triglyceride concentration. Now the reaction will be considered as a three step reversible reaction as it is represented in Figure 27.

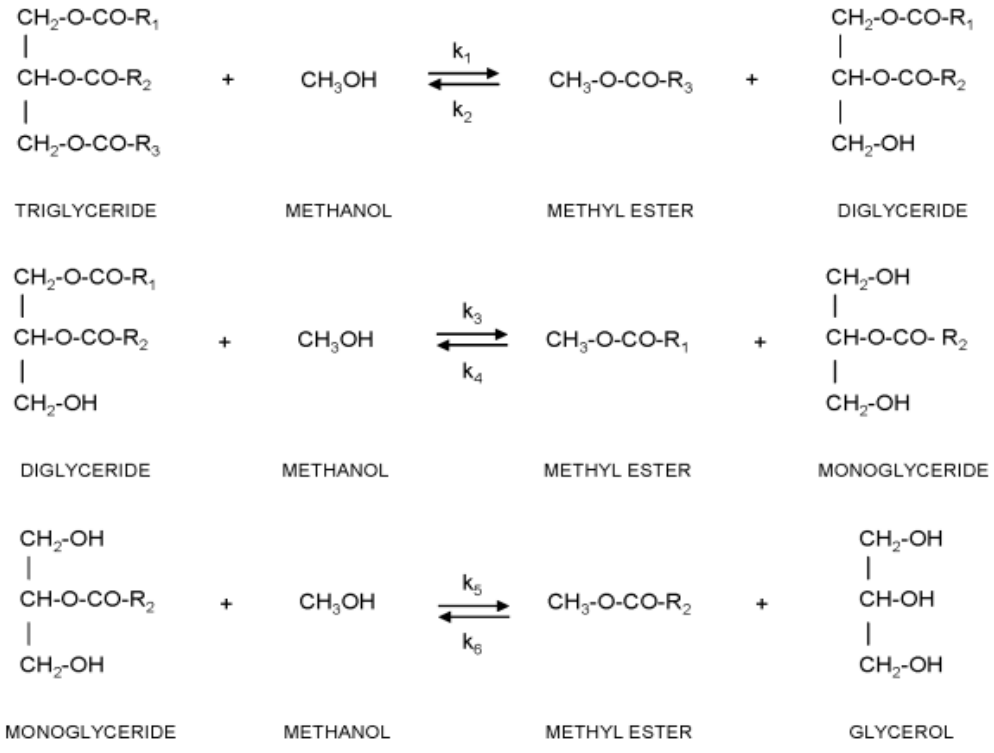

Figure 27: Reactions setps for the transesterifiction of triglycerides

In this kinetic study the three step reversible reactions were considered elementary reactions so there is expected that the forward and reverse reactions to follow second order overall kinetics. Thus mass balance equations regarding each component are as follows:

$$\frac{1}{\rho_{cat}}\frac{dC_T}{d\tau} = -k_1 C_T C_A + k_2 C_E C_D \quad (6.7)$$

$$\frac{1}{\rho_{cat}}\frac{dC_D}{d\tau} = k_1 C_T C_A - k_2 C_E C_D - k_3 C_D C_A + k_4 C_E C_M \quad (6.8)$$

$$\frac{1}{\rho_{cat}}\frac{dC_M}{d\tau} = k_3 C_D C_A - k_4 C_E C_M - k_5 C_M C_A + k_6 C_E C_G \quad (6.9)$$

$$\frac{1}{\rho_{cat}}\frac{dC_G}{d\tau} = k_5 C_M C_A - k_6 C_E C_G \quad (6.10)$$

$$\frac{1}{\rho_{cat}}\frac{dC_E}{d\tau} = k_1 C_T C_A - k_2 C_E C_D + k_3 C_D C_A - k_4 C_E C_M + k_5 C_M C_A - k_6 C_E C_G \quad (6.11)$$

$$\frac{1}{\rho_{cat}}\frac{dC_A}{d\tau} = -k_1 C_T C_A + k_2 C_E C_D - k_3 C_D C_A + k_4 C_E C_M - k_5 C_M C_A + k_6 C_E C_G \quad (6.12)$$

The solution to the kinetic equation system enables to determine the forward and reverse rate constants. In addition the effect of temperature was also studied, and thus plotting the calculated rate constants as a function of temperature the dependence of these values of the temperature was ascertained and the activation energies were determined by the Arrhenius equation:

$$k = k_0 \exp\left(-\frac{E_a}{RT}\right) \quad (6.13)$$

The calculation of the effective rate constants requires the integration of the differential equation system presented, and the subsequent resolution of the resultant equation system. Due to the complexity of the problem, this resolution was carried out using numerical methods. The mathematical program Matlab (The Maths Works Inc.) was used because it has built-in differential equations functions that enable the resolution of ordinary differential equation systems. The code of the program written can be found in appendix to this work.

The resolution method was based on the simulation of the differential equations system starting out with different initial values for the rate constants. The methodology for this resolution consisted in the following steps:

i. As input the range of the six values of rate constants, and the initial value of each one. The values chosen were based on those found in the bibliography[43].
ii. Running the simulation. This is the resolution of the differential equations system, for all the possible combinations of the input values of the reaction rate constants.
iii. Error determination. This meant the comparison between the simulated solutions for the concentrations of the reactants over the space time and the experimental concentrations determined in each sample. The global error was determined as the total number of the absolute errors, i.e., the sum of all vertical distances squared between lines and experimental points of concentration.

iv. Graphical representation of the kinetic model and the experimental results.

Figure 28 shows the product concentration with during the reaction. The methyl ester formation rate increased from the beginning of the reaction until the equilibrium was approached. On the other hand, the concentrations of intermediates-monoglycerides and diglycerides- did not show a significant change. However a slight increase in its concentration was observed during low values of space time, achieving a maximum concentration and then decreasing to nearly zero.

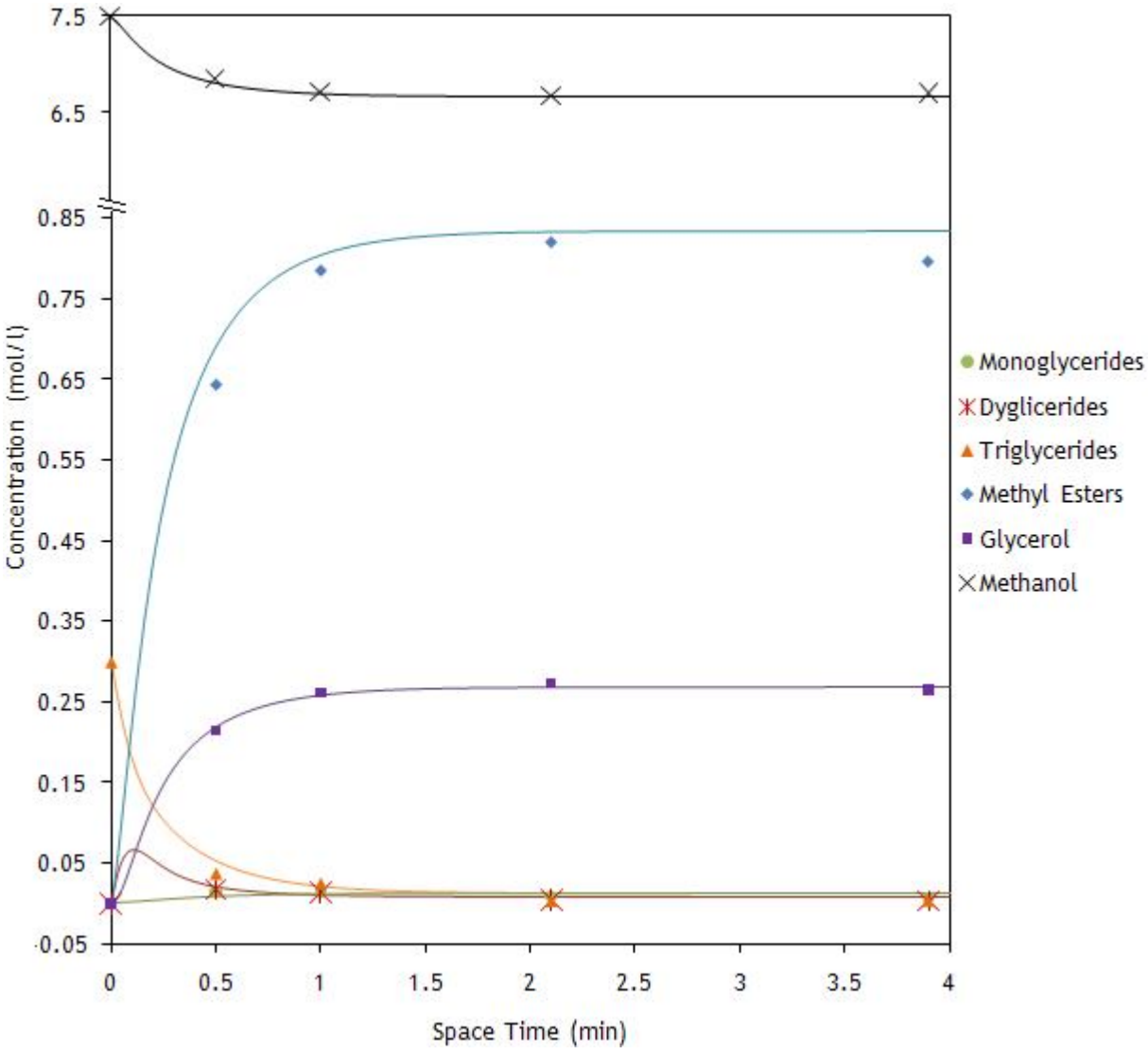

Figure 28: Content of methyl esters, triglycerides, diglycerides, monoglycerides, glycerol and methanol in the products obtained at 205ºC, 250 bar, catalyst mass of 9g, and methanol/oil ratio of 25.

For each of the three temperatures, the above procedure was conducted and the results plotted in a similar way to those shown in Figure 28. Examination of the curve-fitting results showed a good fit of the kinetic model to the experimental results. From the fitting of

the experimental results obtained at three temperatures, the reaction rate constants were calculated and are presented in Table 16.

Table 16: Reaction rate constants determined

Temperature (ºC)	Rate Constants (l.mol^{-1}.min^{-1})					
	k1	k2	k3	k4	k5	k6
150	0.0524	0.245	0.196	7.99	1.24	1.89
180	0.931	3.01	1.22	15.2	29.4	14.2
205	1.51	20.9	3.17	15.7	249	90.3

Reaction rates almost always increase with temperature for elementary irreversible reactions but multiple and reversible reactions occasionally exhibit an optimal temperature with respect to the yield of a desired product. In this case this all the reaction rate constants increased with temperature. The reverse reaction of transformation of monoglycerides and FAMEs into triglycerides and alcohol was the less affected by temperature, being almost insensitive to temperature. The same reaction but in the forward way (Diglyceride to monoglyceride) was enhanced by temperature as was verified to all the other reactions.

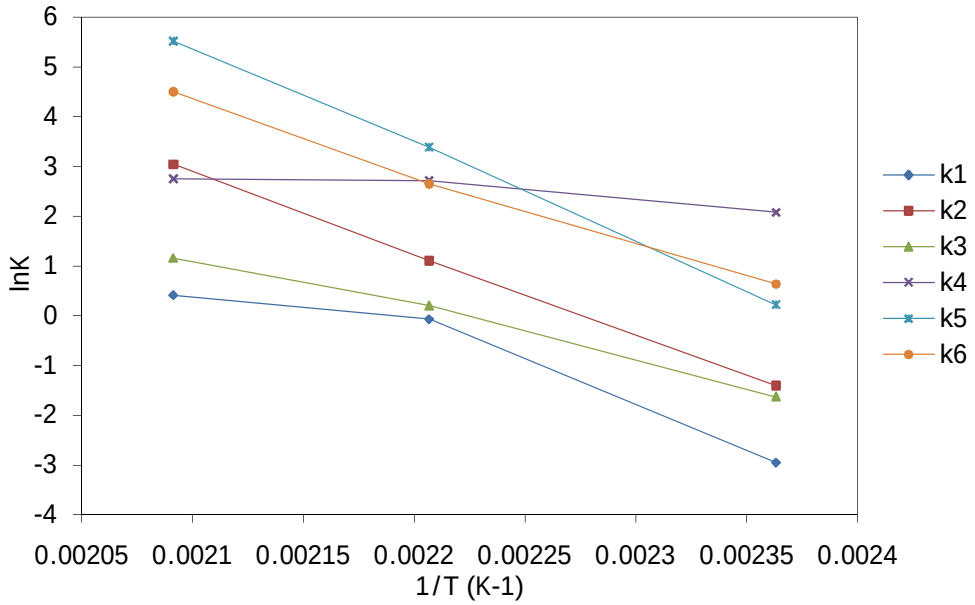

Figure 29: Temperature dependency of the reaction rate constants

In Figure 29 are plotted the reaction rate constants against the inverse of temperature. Using the Arrhenius equation (6.13) the reactions activation energies were calculated and are presented in Table 17. Comparing the results obtained with the work of Noureddini and Zhu(1997)[14] and Vicente et. al (2005)[43], it is verified that the reaction rate values are higher

than those reported and the activations energies are lower. Even most, the mentioned authors performed the reaction in batch mode and with a homogeneous catalyst

Table 17: Determined activation energies for the reactions under study

Reaction	$TG \rightarrow DG$	$DG \rightarrow TG$	$DG \rightarrow MG$	$MG \rightarrow DG$	$MG \rightarrow G$	$G \rightarrow MG$
R^2	0.938	0.996	0.998	0.889	0.999	0.987
k_0	10.24	14.95	8.83	4.78	19.87	14.72
Ea (kj/mol)	16.20	20.48	13.02	3.29	24.56	17.69
Ea (cal/mol)	1.412	5.668	2.79	0.101	6.246	5.41

R^2 , correlation coefficient; k_0-pre exponential constant; Ea- Activation Energy

Comparing these results with those obtained considering a first order single step irreversible reaction, there are obvious differences. Although the reaction rate constants cannot be compared directly, as they are referent to different order reaction rates, the activation energies determined are much lower than the 128 kj/mol value previously determined. This fact makes it clear that for the kinetic study of this reaction, the intermediate species should be included, and a three-step reversible reaction scheme should be considered. Also, in most cases the published work regarding kinetics for single step irreversible reaction considers that the FAMEs percentage is equal to the triglyceride conversion. This is obviously a rough estimation and assumes full conversion of intermediate species, and shouldn't be considered as it leads to different values of reaction rate constants. This is is true even when using a large excess of alcohol, as it is shown is this work, where the use of a molar ratio of methanol to oil of 25 didn't made the reaction irreversible.

The content of free glycerol in each sample, presented in Table 18, in showed that for the samples with high content in FAMEs the glycerol content was below than 0.02% (w/w) which is within the European [17] quality standard for commercial biodiesel, EN 14214. This fact makes a stage of separating and purification unnecessary for the process developed in this work.

Table 18: Free glycerol content in biodiesel samples produced at 205ºC

Space Time (min)	FAMEs % (w/w)	Free Glycerol % (w/w)
0,5	64.0	0,0104
1	78.1	0,0101
2,1	81.6	0,0104
3,9	79.2	0,0123

The kinetic results leads to believe that the conditions in which the reaction was conducted enhanced the transesterification reaction making it a possible route for the biodiesel production in the future.

7 Conclusions

In this thesis the production of biodiesel from sunflower oil was studied in a continuous fixed bed reactor. The transesterification reaction was carried out in supercritical conditions, using carbon dioxide as a co-solvent. The use of the co-solvent enabled the lowering of the reaction mixture critical properties, allowing the use of a solid catalyst, Nafion SAC-13.

Due to the depletion of the world's petroleum reserves and the increasing environmental concerns, there is a great demand for alternative sources of petroleum-based fuel. Biodiesel, a clean renewable fuel has been considered the best candidate for a fuel substite because the possibility to be used in any compression ignition engine, without the need of modifications.

Although the batch process for producing biodiesel allows high flexibility with respect to the composition of the feedstock, it has numeral economic disadvantages: lower equipment productivity and higher operation costs, such as manpower and automation. The productivity can be greatly improved by the implementation of continuous operations. Also, the replacement of a homogeneous catalyst by heterogeneous one is highly advantageous for several reasons: ecological, eliminating the washing section and huge amounts of waste water; economical - cheaper reusable catalyst, production of glycerol and end-product both of high purity; and investment: process simplification and elimination of entire sections from the production schemes.

The work done combines the existing technologies of heterogeneous catalysis and the supercritical process, making the most of the advantages of each one to create a continuous process.

The continuous production of biodiesel under supercritical conditions, using a solid catalyst and carbon dioxide as co-solvent, was accomplished successfully. Results show that the experimental setup assembled allows the production of biodiesel in very short contact times with the catalyst.

The mass transfer between the fluid phase and the solid catalyst was also studied. The mass transfer coefficients were determined using several correlations available in the literature, and the concentration profile between the bulk fluid phase and catalyst surface revealed that, for the operations conditions used, there were no mass transfer limitations. This conclusion goes in agreement to the published claims that the one phase supercritical condition and the presence of co-solvent reduces the transport limitations and increase the reaction rates.

The kinetics of the reaction was also studied, considering the transesterification of sunflower oil as a one-setp irreversible reaction and three-step reversible reaction schemes.

For this a mathematical program was used to adjust the kinetic model to the experimental points. The results showed that, whenever possible, the three step reversible reaction scheme should be consider, as the reversible reactions are important and that they should be accounted for in this process. The determined observed reaction rates and the reaction rates constants were compared to those present in published works. As, so far, it hasn't been reported the heterogeneous catalysis of vegetable oil in supercritical conditions, to the production of biodiesel, so the determined reaction rates and activation energies had to be compared to the conventional cases of heterogeneous catalysis and supercritical production of biodiesel. In both cases the reaction rates were much higher, and the activation energy was found to be similar, 128 kj/mol considering a single irreversible step. The activation energies for each of the reversible reactions were found be lower than those published, what is an indication that the process developed has advantages to the conventional ones.

The chromatographic analysis of the high triglyceride conversion samples produced showed that the glycerol content was below 0.02% (w/w) which a value that is accepted in the quality standards of commercial biodiesel. It is showed that this process, without any stage of separation or purification, can produce biodiesel within the quality standards defined.

The results show that is possible to have a continuous process that results in very high conversion of triglycerides (99.4%) in a very short contact time (2 minutes), and with reasonable fatty acid methyl esters content (82%), making this process a future possibility for the production of biodiesel in a larger scale.

8 Evaluation of the work done

8.1 Accomplished objectives

The objective of this thesis was to combine the existing conventional techniques of the heterogeneous catalysis and the supercritical production of biodiesel, into a continuous process of biodiesel production. This was done successfully.

The thermodynamic study was made to determine the conditions that the reactor should be operated; a co-solvent, carbon dioxide, was added to decrease these values.

It was successfully designed and assembled the continuous experimental setup for the production of biodiesel. Its operation revealed that it was possible to obtain biodiesel with high reaction rates and high conversion of triglycerides.

The analytical method for determination of total and free-glycerol, mono-, di- and triglycerides was successfully implemented in the laboratory, as this chromatography analysis is very sensitive and complex and hadn't been performed before in this laboratory.

A kinetic model was chosen and a Matlab code was written to resolve the differential equation system, and to adjust the kinetic model to the experimental points, and this way determining the reaction rate equations.

In an overall manner it can be said that the project was successful and that all the objectives were accomplished.

8.2 Limitations and suggestions for future work

The limitations of the work done can be divided in three parts:

1. Experimental setup: Although the experimental apparatus allowed the fulfillment of all the objectives proposed had some limitations. The expansion valve used only allowed to change the flow rate in a small range. The suggestion is to use an expansion valve with a lesser valve coefficient; The pump used for the pressurizing of the system and the pumping of the methanol/carbon dioxide should not be a piston pump, but a diaphragm pump, was if possible with buil-in refrigeration. This would allow the removing of the refrigeration bath that was all the inlet tubing were immersed.
2. Operating conditions: To better understand the influence of the operating conditions in the reaction, more experiments should be done using a larger range of flow rates, more temperatures and specially with a higher molar ratio of methanol/oil to increase the FAMEs content in the products.
3. Solid catalyst: Although the external mass transport limitations were studied, the internal mass transfer can play an important role in the final content of FAMEs in the samples. The study should be made, particularly using several sizes of particles to assess the effectiveness of the Nafion SAC-13 catalyst used.

Accessed

9 References

1. *Development of Biodiesel: Current Scenario.* Y.C. Sharma, B.Singh. 13, Renewable and Sustainable Energy Reviews, **2009**. 1646-1651.

2. *Homogeneous, heterogeneous and enzimatic catalysis for transterification of high free fatty acid oil (waste cooking oil) to biodiesel: A review.* M.K. LLam et al, Biotechnology Advances, **2010**.

3. Gerhard Knothe, Jon Van Gerpen, Jurgen Krahl. *The Biodiesel Handobook.* Champaign,Illinois : AOCS Press, **2005**.

4. Directive 2003/30/EC of the European Parliament and of the Council of 8 May 2003 on Promotion of Biofuels or other Renewable Fuels for Transport. .

5. Homepage of the European Biodiesel Borad. : http://www.ebb-eu.org/stats.php. accessed in March 2010

6. Directive 2009/28/EC of the european parliament and of the council of April 2009 on the promotion of the use of energy from renewable sources: http://europa.eu.int/.

7. Wim Soetaert, Erik J.Vandamme. *Biofuels.* : John Wiley & Sons, **2006.**

8. O'brien, Richard D. *Fats and Oils: Formulating and Processing for Applications.* Florida : CRC Press, **2004.**

9. Sonntag. *Structure and Composition of fats and oils. Bailey's Industrial Oil and Fat Products.* New York : Wiley-Interscience, **1979.**

10. Caye M. Drapcho, Nghiem Phu Nhuan, Terry H. Walker. *Biofuels Engineering Process Technology.* New York : McGraw-Hill, **2009.**

11. Pinnarat T., Savage Phillip. *Assessment of Noncatalytic Biodiesel Synthesis Using Supercritical Reaction Conditions.* Ind. Eng. Chem., **2008**, Vol. 47.

12. Dimian A.C., Bildea C.S., *Chemical Process Design*: John Wiley & Sons, **2008**

13. Vujicic Dj. et al, *Kinetics of Biodiesel from sunflower oil over CaO heterogeneous catalyst.* Fuel, **2010**

14. Zuh D., Noureddini H., *Kinetics of Transesterification of Soybean Oil.* Biocatalyst articles, **1997.**

15. Bournay L., Casanav D., Delfort B.,Hillion G. ,Chodorge ,J.A., *New heterogeneous process for biodiesel production* , Catal. Today . **2005**

16. Cao,W.; Han.; Zhang, J. Fuel, **2005**

17. Standard UNE-EN 14103: *Determination of ester and linolenic acid methyl ester contents, issued by Asociación Española de Normalización y Certificación*, Madrid, **2003.**

18. Han, H.; Cao, W.; Zhang, J. Process Biochemestry, **2005**

19. Bertoldi C. et al, *Continuous Production of Biodiesel from soybean Oil in Supercritical Ethanol and Carbon dioxide as co-solvent*, Energy & Fuels, **2009**

20. Weber W., Petrov S., Brunner G., Fluid Phase Equil., Vol. 58-160, **1999**

21. Reid, R., Prausnitz, B. y B., Poling. *The properties of gases and Liquids 4th ed.* New York : McGraw Hill, **1987.**

22. B. E Poling, J. M. Prausnitz, J. P. O'Connel, *The properties of Gases and Liquids 5th edition, McGraw-Hill*, New York, **2001**

23. Pfohl, O., S. Petkov, and G. Brunner, PE 2000: *A Powerful Tool to Correlate Phase Equilibria, Herbert Utz Verlag,* Munich **2000.**

24. McHugh M., and V. Krukonis, Supercritical Fluid Extraction, 2nd Edition,Butterworth–Heinemann, Stoneham, UK **1994.**

25. Sandler , *Chemical and Engineering Thermodynamics, 3rd Edition*, Wiley, New York **1999**.

26. Hougen, O. A., K. M. Watson, and R. A. Ragatz, Principios de los procesos quıímicos, Vol. 2, Editorial Reverte´, S. A., Madrid, **1954**.

27. M.A. Harmer, Q. Sun. Applied Catalysis A.Gen., Vol. 221.

28. Santana A., Ramírez E., Larrayoz M.A., Recasens F., M*ethodology for Screening of Modifiers for Single-Phase Vegetable Oil Hydrogenation in SC CO2: Transesterification of Sunflower Oil for Biodiesel Production Supercritical Alcohols: A Preliminary Phase Equilibria Study*. II Iberoamerican Conference on Supercritical Fluids-Natal (Brasil) p. 75 **2010**

29. Santana A., Ramírez E., Recasens F., Larrayoz M.A., *A Phase Equilibria Study of Sunflower oil Tranesterification using Supercritical Alcohols with carbon dioxide as Cosolvent. 12th European Meeting on Supercritical Fluids* , Graz (Austria) p.121 **2010**

30. *Transesterification of triacetin with methanol on Nafion acid resins.* Dora E. Lépoz, James Goodwin Jr, David A. Bruce. 381-391, s.l. : Journal of Catalysis, **2007**

31. *Esterification of free fatty acis in sunflower oil over solid catalysts using batch and fixed bed-reactors.* J. Ni, F.C. Meunier Applied Catalysis A, **2007**

32. *Transesterification kinetics of soybean oil.* Freedman, B, Butterfield, R.O y Pryde, J. Am. Oil Chem. Soc. , **1986**

33. *Assessment of Noncatalytic Biodiesel Synthesis Using Supercritical Reaction Conditions.* **T.,** Pinnarat y P.E., Ind. Eng. Chem. Res., **2008**

34. *Chemical ReactorAnalysis and Design.* G.F., Froment y K.B., Bischoff. New York : Wiley, **1979.**

35. Montgomery, Design and Analysis of Experiments (6 ed.), John Wiley & Sons, Inc., New York **2005**

36. A. Valle, T.F. Rezende, R.A. Souza, V.M.D. Pasa and I.C.P. Fortes, Combination of Fractional and Doehlert experimental designs in biodiesel production: ethanolysis of Raphanus sativus L. var. oleiferus Stokes oil catalyzed by sodium ethoxide, Energy & Fuels 23**, 2009**

37. *Kinetics oftransesterification in rapeseed oil to biodiesel fuels as treated in supercritical methanol.* Kusdiana, D. y Saka, S. 693-698, s.l. : Fuel, **2001**, Vol. 80.

38. G., Brunner**.** *Gas Extraction: An Introduction to Fundamentals of Supercritical Fluids and the Application to Separation Processes.* New York : Springer, **1994.**

39. Wakau, N.; Kaguei, S. *Heat and Mass Transfer in Packed Beds*; Gordon and Breach: New York, **1982**

40. Lim, G. B.; Holder, G. D.; Shah, Y. T. Mass Transfer in Gas-Solid Systems at Supercritical conditions. *J. Supercrit. Fluids* **1990**

41. Tan, C. S.; Liang, S. K.; Liou, D. C. Fluid-Solid Mass transfer in a Supercritical Fluid Extractor. *Chem. Eng. J.* **1988**,38, 17.

42. Levenspiel O., *Chemical Reaction engineering*, 3rd Edition, Josh Wiley & Sons, **1999**

43. G. Vicente, M Martínez, J. Aracil, A. Esteban. ,Ind. Eng. Chem. Res., **2005**

44. M.K. Lam, K.T. Lee, A.R. Mohamed, *Homogeneous, heterogeneous and enzimatic catalysis for transesterification of high free fatty acid oil (waste cooking oil) to biodiesel: A review.* Biotechnology Advances , **2010.**

10 Appendix

A- *Vegetable oils: Oil content, Yield, and Producing Areas*

Oil	Oil Content (%)	Oil Yield (Pounds/Acre)	Producing Areas
		Oil seeds:	
Canola	40 - 45	525-590	Canada, China, India, France, Austria, United Kingdom, Germany, Poland, Denmark, Czechoslovakia, United States
Corn	3.1- 5.7	215-390	United States, Mexico, Canada, Japan, China, Brazil, South Africa, Argentina, Russia, Commonwealth, of Independent States (CIS), Belgium, France, Italy, Germany, Spain, United Kingdom
Cottonseed	18 - 20	185-210	China, Russia, United States, India, Pakistan, CIS, Brazil, Egypt, Turkey, Australia
Peanut	45 - 50	1120-1245	China, India, Nigeria, Unietd States, Senegal, South Africa, Argentina
Safflower	30 - 35	545-635	China, United States, Spain, Portugal
Soybean	18 - 20	400-450	United States, Brazil, Argentina, China, India, Paraguay, Bolivia
Sunflower	35 - 45	450-590	Russia, Argentina, CIS, Austria, France, Italy, Germany, Spain, United States, United Kingdom
		Tree fruits and kernels:	
Coconut	65-68	650-870	Philippines, Indonesia, India, Mexico, Sri Lanka, Thailand, Malaysia, Vietnam, Mozambique, New Guinea, Ivory Coast
Olive	15-35	90-260	Spain, Italy, Greece, Tunisia, Turkey, Morocco, Portugal, Syria, Algiers, Yuguslavia, Cyprus, Egypt, Israel, Libya, Jordan, Lebanon, Argentina, Chile, Mexico, Peru, United States, Australia
Palm	45-50	2670-4450	Malaysia, Indonesia, China, Philippines, Pakistan, Mexico, Bangladesh, Colombia, Ecuador, Nigeria, Ivory Coast
Palm kernel	44-53	267-445	Malaysia, Indonesia, China, Philippines, Pakistan, Mexico, Bangladesh, Colombia, Ecuador, Nigeria, Ivory Coast

B- Estimation of the Thermodynamic properties of the mixture Methanol/CO_2

B.1 Mixture critical temperature

The true critical temperature is usually not a linear mole fraction average of the true component critical temperatures. Li (1971) has suggested that if the composition is expressed as

$$\emptyset_j = \frac{y_i}{\sum_i y_i V_{ci}} \tag{B.1}$$

the true mixture critical temperature can be estimated by

$$T_{cT} = \sum_j \emptyset_j T_{cj} \tag{B.2}$$

where y_i is the mole fraction of component j, V_{cj} is the critical volume of component j, T_{cj} is the critical temperature of j, and T_{cT} is the true critical temperature of the mixture.

Chueh and Prausnitz (1967) have proposed a similar technique by defining a surface fraction θ_j :

$$\theta_j = \frac{y_i V_{cj}^{2/3}}{\sum_i y_i V_{ci}^{2/3}} \tag{B.3}$$

they then relate θ_j and T_{cj} by

$$T_{cT} = \sum_j \theta_j T_{cj} + \sum_i \sum_j \theta_i \theta_j \tau_{ij} \tag{B.4}$$

where $\tau_{ij}$is an interaction parameter. $\tau_{ii}$is considered to be zero, and τ_{ij} ($i \neq j$) can be estimated for several different binary types by

$$\psi_T = A + B\delta_T + C\delta_T^2 + D\delta_T^3 + E\delta_T^4 \tag{B.5}$$

Where

$$\psi_T = \frac{2\tau_{ij}}{T_{ci}+T_{cj}} \tag{B.6}$$

and

$$\delta_T = \left|\frac{T_{ci}-T_{cj}}{T_{ci}+T_{cj}}\right| \tag{B.7}$$

The coefficients for Eq. A.5 are shown in Table A.1, where $0 \leq \delta_T \leq 0.5$:

Table B.1. Coefficients for equation A.5 (Reid *et al*., 1987)

Binary	A	B	C	D	E
Containing aromatics	-0.0219	1.227	-24.277	147.673	-259.433
Containing H_2S	-0.0479	-5.725	70.974	-161.319	
Containing CO_2	-0.0953	2.185	-33.985	179.068	-264.522
Containing C_2H_2	-0.0785	-2.152	93.094	-722.676	
Containing CO	-0.0077	-0.095	-0225	3.528	
All other systems	-0.0076	0.287	-1.343	5.433	-3.038

Using the equations given above, the critical temperature of the methanol/CO2 mixture was estimated by both Li(1971) and Chueh-Prausnitz (1967) methods. The coefficients and temperatures determine are presented in table B.2 and B.3.

Table B.2. Critical temperature for the Methanol/CO_2 mixture using the Li (1971) method

Molar composition (% methanol)	Ø Methanol	ØCO_2	Mixture critical temperature (K)
0,05	0,0620	0,9380	317,03
0,10	0,1225	0,8775	329,65
0,15	0,1815	0,8185	341,94
0,20	0,2391	0,7609	353,94
0,25	0,2952	0,7048	365,65
0,30	0,3500	0,6500	377,08
0,40	0,4559	0,5441	399,15
0,50	0,5569	0,4431	420,21

Table B.3. Critical temperature for the Methanol/CO_2 mixture using the Chueh and Prausnitz (1967) method

Molar composition (% methanol)	θ Methanol	θ CO_2	δ_T	ψ_T	ξ_T	Mixture critical temperature (K)
0,05	0,0578	0,9422	0,2553	0,1034	42,2197	320,74
0,10	0,1146	0,8854	0,2553	0,1034	42,2197	336,55
0,15	0,1705	0,8295	0,2553	0,1034	42,2197	351,58
0,20	0,2255	0,7745	0,2553	0,1034	42,2197	365,86
0,25	0,2796	0,7204	0,2553	0,1034	42,2197	379,41
0,30	0,3329	0,6671	0,2553	0,1034	42,2197	392,27
0,40	0,4370	0,5630	0,2553	0,1034	42,2197	416,00
0,50	0,5380	0,4620	0,2553	0,1034	42,2197	437,26

B.2 Mixture critical volume

Only a few experimental values are available for mixture critical volumes. Thus the range and accuracy of estimation methods are not clearly established. Grieves and Thodos (1963) have suggested an approximate graphical method for hydrocarbon mistures, but an analytical techinique by Chueh and Prausnitz (1967), modified by Schick and Prausnitz (1967) appears to be more accurate, accordingly to Reid *et al.* (1987). When the surface fraction θ_j is defined as in Eq. A3, the mixture critical volume is given by a relation analogous to equation A.4:

$$V_{cT} = \sum_j \theta_j V_{cj} + \sum_i \sum_j \theta_i \theta_j v_{ij} \quad \text{(B.8)}$$

V_{cj} is the critical volume of j, and v_{ij} is an interaction parameter such that $v_{ii} = 0$ and v_{ij} $(i \neq j)$ can be estimated as follows:

$$\psi_v = A + B\delta_v + C\delta_v^2 + D\delta_v^3 + E\delta_v^4 \quad \text{(B.9)}$$

$$\psi_v = \frac{2v_{ij}}{V_{ci}+V_{cj}} \quad \text{(B.10)}$$

$$\delta_v = \left| \frac{V_{ci}^{2/3} - V_{cj}^{2/3}}{V_{ci}^{2/3} + V_{cj}^{2/3}} \right| \quad \text{(B.11)}$$

The coefficients for Eq. B.9 are given in the Table B.4 when $0 \leq \delta_v \leq 0.5$.

Table B4. Coefficients for equation B.9 (Reid *et al.*, 1987)

Binary	A	B	C	D	E
Aromatic-aromatic	0	0	0	0	0
Containing at least one cycloparaffin	0	0	0	0	0
Paraffin-aromatic	0.0753	-3.332	2.220	0	0
System with CO_2 or H_2S	-0.4957	17.1185	-168.56	587.05	-698.89
All other systems	0.1397	-2.9672	1.8337	-1.536	0

Using the equations stated above, the critical volume of the methanol/CO_2 mixture was estimated, for several molar compositions of the mixture. The results are presented in Table B.5.

Table B.5. Critical volume for the methanol/CO_2 mixture

Molar Composition (% Methanol)	θ Methanol	θ CO_2	δ_U	ψ_U	ζ_U	Mixture critical volume (cm^3/mol)
0,05	0,0578	0,9422	0,0760	0,0661	7,0022	96,05
0,10	0,1146	0,8854	0,0760	0,0661	7,0022	98,08
0,15	0,1705	0,8295	0,0760	0,0661	7,0022	99,99
0,20	0,2255	0,7745	0,0760	0,0661	7,0022	101,78
0,25	0,2796	0,7204	0,0760	0,0661	7,0022	103,46
0,30	0,3329	0,6671	0,0760	0,0661	7,0022	105,03
0,40	0,4370	0,5630	0,0760	0,0661	7,0022	107,88
0,50	0,5380	0,4620	0,0760	0,0661	7,0022	110,35

A.3 Mixture critical pressure

The dependence of mixture critical pressures on mole fraction is often non linear, and estimation of P_{cT} is often unreliable. One method generally accepted to estimate the critical pressure, was developed by Chueh and Prausnitz (1967). The critical pressure of the mixture was related to the critical temperature and pressure by a modified Redlich-kwong equation of state (Reid *et al.*, 1987):

$$P_{cT} = \frac{RT_{cT}}{V_{cT}-b_m} - \frac{a_m}{T_{cT}^{1/2}V_{cT}(V_{cT}+b_m)} \quad \text{(B.12)}$$

where T_{cT} and V_{cT} are calculated form methods described earlier in this section. The mixture coefficients for determining P_{cT} are defined as follows:

$$b_m = \sum_j y_j b_j = \sum_j \frac{y_j \Omega_{bj}^* RT_{cj}}{P_{cj}} \quad \text{(B.13)}$$

$$a_m = \sum_i \sum_j y_i y_j a_{ij} \quad \text{(B.14)}$$

with

$$\Omega_{bj}^* = 0.0867 - 0.0125w_j + 0.011w_j^2 \quad \text{(B.15)}$$

$$a_{ii} = \frac{\Omega_{ai}^* R^2 T_{ci}^{2.5}}{P_{ci}} \quad \text{(B.16)}$$

$$a_{ij} = \frac{(\Omega_{ai}^* + \Omega_{aj}^*) RT_{cij}^{1.5}(V_{ci}+V_{cj})}{4[0.291-0.04(\omega_i-\omega_j)]} \quad \text{(B.17)}$$

$$T_{cij} = (1 - k_{ij})\sqrt{T_{ci}T_{cj}}$$

$$\Omega^*_{aj} = \left(\frac{RT_{cj}}{V_{cj}-b_j} - P_{cj}\right)\frac{P_{cj}V_{cj}(V_{cj}+b_j)}{(RT_{cj})^2} \quad \text{(B.18)}$$

The interaction parameter usually ranges from 0.1 to 0.01. Values for a large number of binary system have been tabulated (Chueh and Prausnitz, 1967). In Table B.6 the estimated value of critical pressure is presented for several molar compositions of the mixture methanol/carbon dioxide.

Table B6. Critical Pressure for the methanol/CO_2 mixture

Molar Composition (% Methanol)	Ω^*_b (CH_4O)	Ω^*_b (CO_2)	b (CH_4O)	b (CO_2)	b_m (mixture)	Ω^*_a (CH_4O)	Ω^*_a (CO2)
0,05	0,0832	0,0843	43,8031	28,8940	29,6395	0,4197	0,4195
0,10	0,0832	0,0843	43,8031	28,8940	30,3849	0,4197	0,4195
0,15	0,0832	0,0843	43,8031	28,8940	31,1304	0,4197	0,4195
0,20	0,0832	0,0843	43,8031	28,8940	31,8758	0,4197	0,4195
0,25	0,0832	0,0843	43,8031	28,8940	32,6213	0,4197	0,4195
0,30	0,0832	0,0843	43,8031	28,8940	33,3667	0,4197	0,4195
0,40	0,0832	0,0843	43,8031	28,8940	34,8577	0,4197	0,4195
0,50	0,0832	0,0843	43,8031	28,8940	36,3486	0,4197	0,4195

Table B7. Critical pressure for the methanol/CO_2 mixture (continuation)

Molar Composition (% Methanol)	a (CH_4O/CH_4O)	a (CO_2/CO_2)	Tc (CH_4O/CO_2)	a (CH_4O $/CO_2$)	a_m (mixture)	Mixture critical pressure (bar)
0,05	$2,13x10^8$	$6,34x10^7$	$3,69x10^2$	$1,01x10^8$	$6,73x10^7$	90,20
0,10	$2,13x10^8$	$6,34x10^7$	$3,69x10^2$	$1,01x10^8$	$7,16\ x10^7$	103,43
0,15	$2,13x10^8$	$6,34x10^7$	$3,69x10^2$	$1,01x10^8$	$7,63\ x10^7$	114,01
0,20	$2,13x10^8$	$6,34x10^7$	$3,69x10^2$	$1,01x10^8$	$8,14\ x10^7$	122,30
0,25	$2,13x10^8$	$6,34x10^7$	$3,69x10^2$	$1,01x10^8$	$8,68\ x10^7$	128,63
0,30	$2,13x10^8$	$6,34x10^7$	$3,69x10^2$	$1,01x10^8$	$9,27\ x10^7$	133,24
0,40	$2,13x10^8$	$6,34x10^7$	$3,69x10^2$	$1,01x10^8$	$1,05\ x10^8$	138,01
0,50	$2,13x10^8$	$6,34x10^7$	$3,69x10^2$	$1,01x10^8$	$1,20\ x10^8$	137,77

C-Equipment list

Sunflower Oil Pump
- Gilson, HPLC pump model 305; Q-ratemax = 10ml/min; ΔPmax = 62 MPa ;

SC Solvent Pump
- Maximator model M111D-327

Thermocouples
- Type K, Stainless Steel

Pressure Gauges
- Wika, plastic dial cover/solid front stainless steel case

Rupture Disc
- Autoclave Engineers, Stainless Steel, Pmax = 35 MPa

Relief Valves
- Haskel, model 27741-6, Stainless Steel body, Pmax = 35 MPa

Expansion Valve
- Autoclave Engineers Needle valve, model 10VRMM2812, Stainless Steel, Tmax = 403.15 at 30 MPa; Cvmax = 0.004

Air Compressor
- ABAC model B4900LN/T4, 514 l/min at 1.1 MPa

Pressure Regulators
- GO, Model PR57, Stainless Steel body, Pmax = 69 MPa

Static Mixer
- Kenics, model 37-04-065, 20 cm long, ¼ in. OD, Pmax = 24 MPa at 423.15 K

Pre-heater
- Kosmon S.A., model 43000, Stainless Steel, Tmax = 545.15 K, Pmax = 30 MPa, 600W

Reactor Pressure Gauge
- Autoclave Engineers, K-Monel Bourdon tube

Reactor Thermowell
- Autoclave Engineers, Hastelloy C, type K

Titanium Reactor
- Eurotechnica, HPA 500. Tmax = 523.15 K at 50 MPa, ID = 17.5 mm, inner length = 152 mm

Control Thermostat
- Huber, model 230, thermoregulation liquid = ethylene glycol-water (40%v/v), temperature range= 243.15 – 473.15 K, volume 5 l

Rotameter
- Tecfluid, model 2300, 20-140 l/h C3H8, Tmax = 393.15 K, Pmax = 1.5 MPa

D- Response Surface Regression: FAMEs versus Temperature; Space Time

D1. Experimental conditions studied: Central composite design

Table D1: Experimental conditions studied: Central composite design

Run	Real Values		Coded Values	
	Temperature (ºC)	Space Time (min)	X_T	X_τ
1	180	0,5	0,091	-1,000
2	180	2,1	0,091	-0,030
3	205	2,1	1,000	-0,030
4	150	0,5	-1,000	-1,000
5	205	3,9	1,000	1,061
6	180	3,9	0,091	1,061
7	180	1	0,091	-0,697
8	205	0,5	1,000	-1,000
9	150	1	-1,000	-0,697
10	150	3,9	-1,000	1,061
11	205	1	1,000	-0,697
12	150	2,1	-1,000	-0,030

D2. Response Surface Regression

```
The analysis was done using coded units.

Estimated Regression Coefficients for FAMEs %

Term                                     Coef  SE Coef       T      P
Constant                               70,295    4,869  14,438  0,000
Temperature ( ºC)                      27,639    3,131   8,828  0,000
Space Time (min)                       13,167    3,213   4,098  0,005
Temperature ( ºC)*Temperature ( ºC)   -12,966    5,041  -2,572  0,037
Space Time (min)*Space Time (min)     -11,867    5,329  -2,227  0,061
Temperature ( ºC)*Space Time (min)     -4,343    3,869  -1,122  0,299


S = 8,66490    PRESS = 1699,07
R-Sq = 94,41%  R-Sq(pred) = 81,91%  R-Sq(adj) = 90,41%


Analysis of Variance for FAMEs %

Source          DF   Seq SS   Adj SS   Adj MS      F      P
Regression       5  8868,33  8868,33  1773,67  23,62  0,000
  Linear         2  7763,12  7154,34  3577,17  47,64  0,000
  Square         2  1010,62  1011,70   505,85   6,74  0,023
  Interaction    1    94,59    94,59    94,59   1,26  0,299
Residual Error   7   525,56   525,56    75,08
```

```
  Lack-of-Fit    6   525,56   525,56    87,59      *      *
  Pure Error     1     0,00     0,00     0,00
Total           12  9393,89
```

```
Unusual Observations for FAMEs %

Obs  StdOrder  FAMEs %     Fit  SE Fit  Residual  St Resid
  1         7   32,500  48,062   5,625   -15,562     -2,36 R

R denotes an observation with a large standardized residual.
```

```
Estimated Regression Coefficients for FAMEs % using data in uncoded units

Term                                      Coef
Constant                               -722,092
Temperature ( ºC)                       7,29714
Space Time (min)                        43,7116
Temperature ( ºC)*Temperature ( ºC)  -0,0171445
Space Time (min)*Space Time (min)       -4,35875
Temperature ( ºC)*Space Time (min)   -0,0957139
```

Response Optimization

```
Parameters
         Goal     Lower  Target  Upper  Weight  Import
FAMEs %  Maximum     80     100    100       1       1


Starting Point
Temperature    =   150
Space Time (   =   0,5


Global Solution
Temperature    =       205
Space Time (   =   2,76667


Predicted Responses
FAMEs %   =   86,6085  ,   desirability =   0,330423
Composite Desirability = 0,330423
```

E. Chromatography Analysis

E.1 Analysis of FAMEs content

The protocol for the analysis of FAMEs in the reaction samples was based on the European standard method EN 14103, and is described in the following lines:

- Transfer a part of the upper phase of the biodiesel sample produced to a screw cap vial and close it hermetically to prevent humidity in the sample; store the vials in the freezer.
- Prepare vials with 5 mL of a 10 mg/L methyl hetpadecanoate solution previously prepared and seal each vial hermetically.
- Using a micro syringe transfer 250 mg of the sample stored previously , to the vial with the methyl heptadecanoate solution; wrap the sealing of the vial with parafilm to prevent evaporation of the solvent n-heptane; the sample is ready for injection.
- After the operating conditions of the chromatograph are reached, and its signal is stabilized inject 1 µL of the prepared solution, and start the acquisition program on the PC.
- Before and after each injection clean the syringe seversl times with n-heptane.

The ester content, expressed as a mass fraction in percent is calculated by the following expression:

$$C = \frac{(\sum A) - A_{EI}}{A_{EI}} x \frac{C_{EI}\, x\, V_{EI}}{m} x100\% \qquad (3.4.1)$$

Where:

- $\sum A$ is the total peak area from the methyl ester in C_{14} to that in $C_{24:1}$;
- A_{EI} is the peak area corresponding to methyl hetpadecanoate;
- C_{EI} is the concentration, in milligrams per millilitre, of the methyl hetpadecanoate solution being used;
- V_{EI} is the volume, in millilitres, of the methyl hetpadecanoate solution being used;
- m is the mass in, milligrams, of the sample.

In the next figure is presented an chromatogram of a biodiesel sample produced.

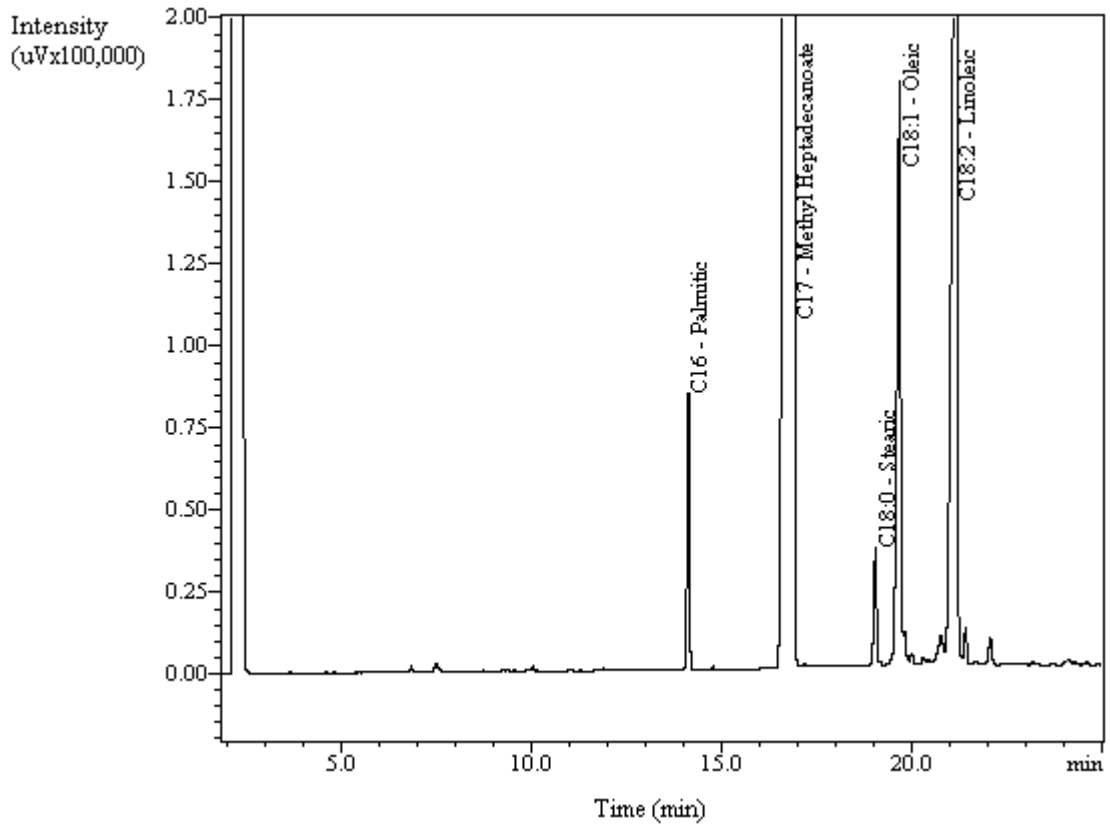

Figure E.1.: Chromatogram obtained from analysis of an experimental sample produced

E.2 Analysis of the mono-,di- and triglycerides content

This chromatographic analysis was carried out under the EN14105 European Standard. In the following lines are presented the formulas to determine the content of each component and the calibrations functions obtained.

Calculation of the free glycerol

$$G = \left[ag\left(\frac{Ag}{Aei1}\right) + bg\right]x\left(\frac{Mei1}{m}\right)x100$$

Where

G is the percentage (m/m) of free glycerol in the sample;

Ag is the peak area of the glycerol

Aei1 is the peak area of internal standard No.1

Mei1 is the mass of internal standard No.1 (milligrams)

m is the mass of sample (milligrams)

Ag and bg are consts coming from regression method for glycerol

Calculation of the glycerides

$$M = am(\sum Ami/Aei2) + bm]\ x\ (Mei2/m)x100$$

$$D = ad(\sum Adi/Aei2) + bd]\ x\ (Mei2/m)x100$$

$$T = at(\sum Ati/Aei2) + bt]\ x\ (Mei2/m)x100$$

Where

M,D, T are the mono-, di- and triglycerides percentage (m/m) in the samples

$\sum Ami$, $\sum Adi$, $\sum Ati$, are the sums of the peak areas of the mono-, di and triglycerides

Aei2 is the peak area o finternal standard No.2

Mei2 is the mass of interna starndar No.2

m is the mass of sample (milligrams)

am and *bm* are constants coming from regression method for monoglycerides

ad and *bd* are constants coming from regression method for diglycerides

at and *bt* are constants coming from regression method for triglycerides

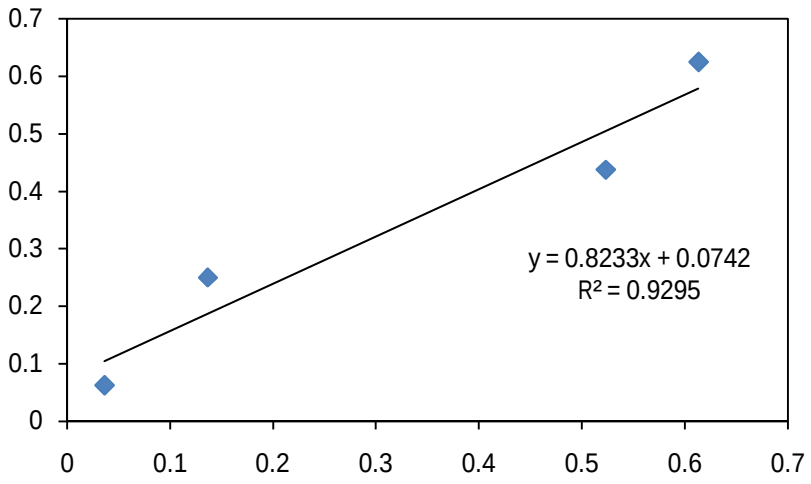

Figure E.1. Free Glycerol calibration curve.

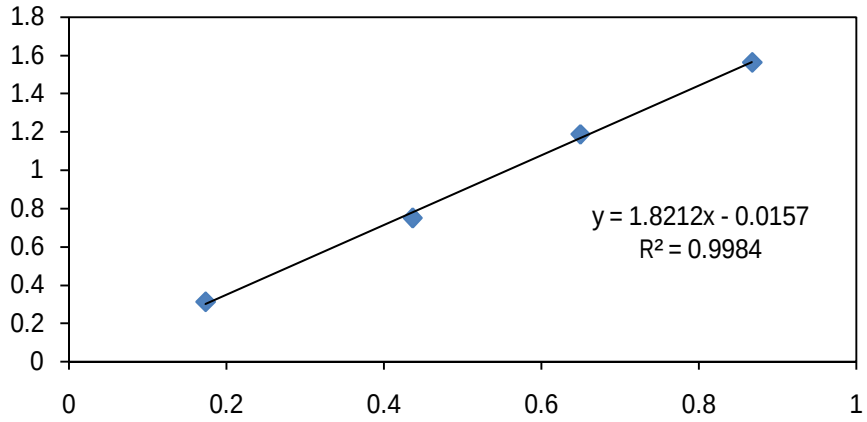

Figure E2. Monoleín calibration curve

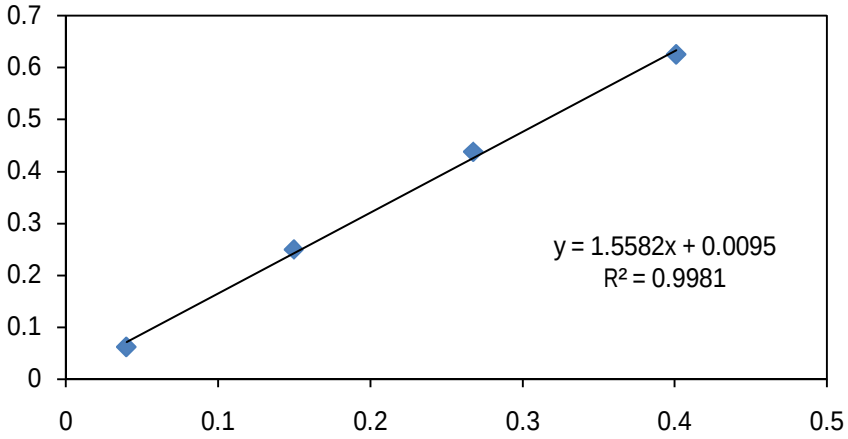

Figure E.3 diolein calibration Curve

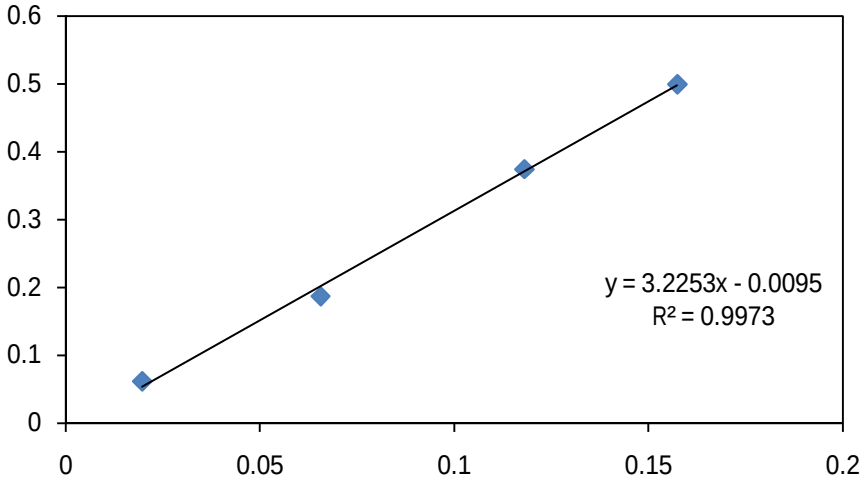

Figure E.4. Trioelin Calibration Curve

From the calibration curves the parameters a and b were dtermined and are presented in the following table.

Table E.1. Determined coeficients of the glycerides calibration curves

Parameter	Triglyceride	Diglyceride	Monglyceride	Glycerol
a	3.2253	1.558	1.821	0.823
b	0.0095	0.0095	0.0157	0.074

In the next picture is preseneted one of the chromatagrams obtained during the analysys of the biodiesel samples.

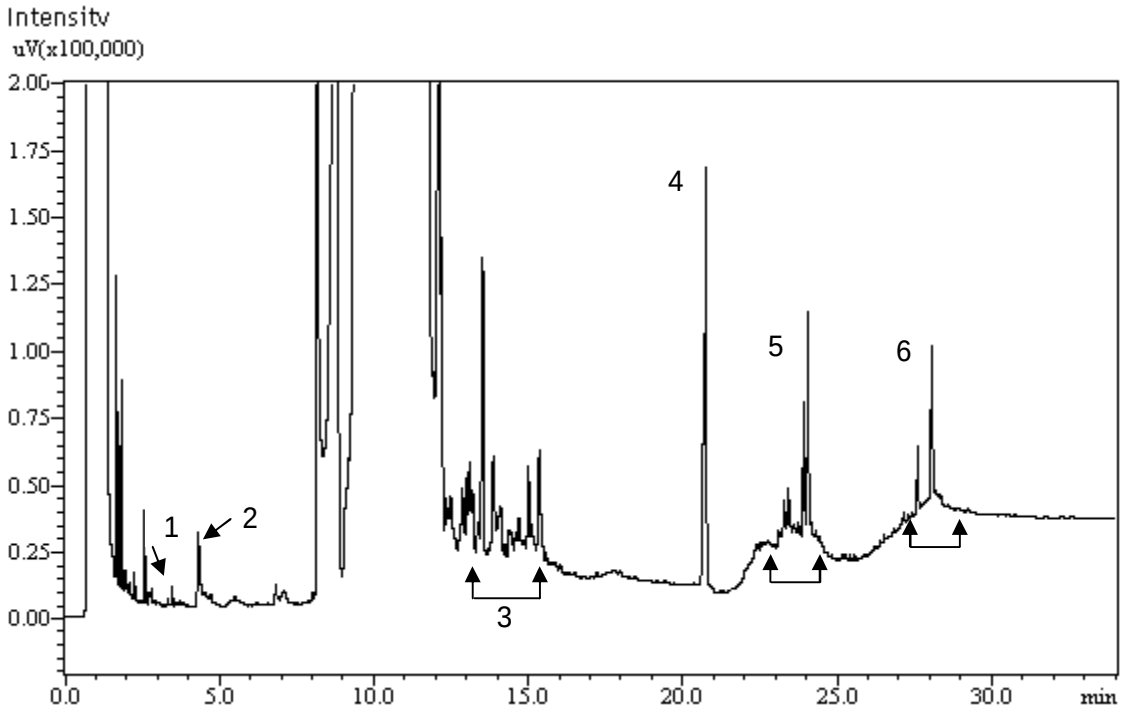

E.2 Chromatogram of one of the samples analyzed. Details of mono-, di-, and triglycerides peaks: 1- Glycerol; 2-Butanetriol IS1; 3-Monoglycerides; 4-Tricaprin IS2; 5- Diglycerides; 6 – Triglycerides.

F- Catalyst properties

Table F1: Physicochemical characteristics of Nafion® SAC-13

Parameter	Nafion® SAC-13
Support	SiO_2
Composition	Fluorosulfonic acid Nafion® polymer (10-20 wt%) on amorphous silica (porous nanocomposite)[a]
Acidic group	$-CF_2CF_2SO_3H$
Ionic form	H^+
Exchange capacity	120-1000 µeq/g [a]
Pellet shape	Lobular, lengthwise striations
Pellet size	+20 mesh (diameter ~ 1mm, length/diameter =9.4
Pore volume	>0.6 mL/g [a]
Pore diameter	>10 nm [a]
Bulk density	0.4-0.5 g/mL [a]
Polymer density	2.1 g/mL [a]
Surface Area	>200 m^2/g [a]
Max. operating temperature	220 ºC [a]

[a] General information provided by the manufacturer

G- Determination of the mixture density – Pen Robinson equation

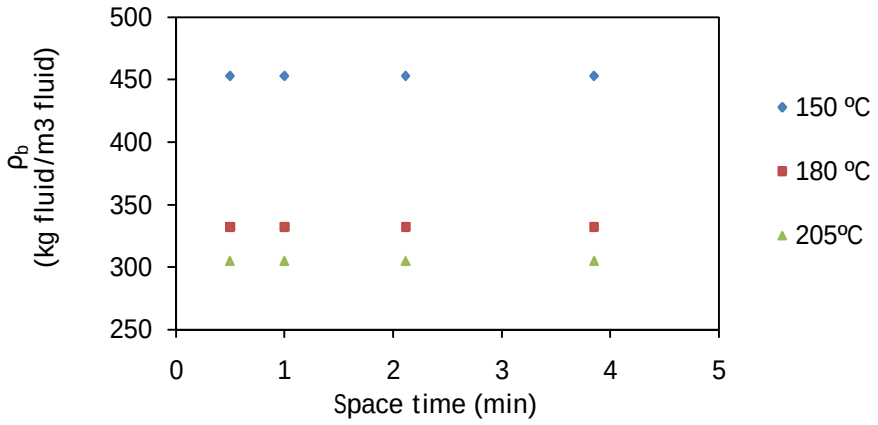

Figure G1: Bulk density calculated to each experiment done

H- Influence of the temperature in the mass transfer coefficients

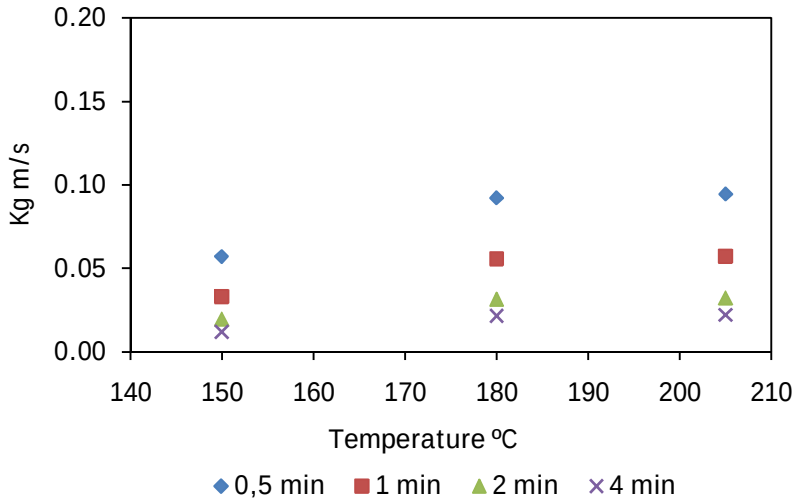

Figure H1: Values of the mass transfer coefficients in function of temperature and space time inside the reactor

I. Determination of the mixture viscosity

Table I1. Carbon Dioxide viscosity at 250 bar and several temperatures

P (bar)	T(K)		μP	Viscosity kg/ms	g/(cm.s)
250	150	423,15	380	0,000038	3,80E-06
	180	453,15	320	0,000032	3,20E-06
	205	478,15	325	0,0000325	3,25E-06

Table I2. Methanol viscosity at 1 and 250 bar and several temperatures

P (bar)	T(K)		cP	Viscosity kg/ms	g/(cm.s)
1,01325	25	298,15	0,55	5,50E-04	5,50E-05
	150	423,15	0,13	1,33E-04	1,33E-05
	180	453,15	0,10	1,02E-04	1,02E-05
	205	478,15	0,08	8,21E-05	8,21E-06
250	25	298,15	0,55	5,50E-04	5,50E-05
	150	423,15	0,67	6,70E-04	6,70E-05
	180	453,15	0,44	4,44E-04	4,44E-05
	205	478,15	0,33	3,25E-04	3,25E-05

Table I3. Mixture carbon dioxide / methanol viscosity g/(cm.s)

Mixture Composition	
Y_{CO2}	0,75
Y_{MeOH}	0,25
Temperature	Viscosity
150ºC	7,79E-06
180ºC	6,18E-06
250ºC	5,78E-06

H. Diffusion calculations

The diffusion coefficient was estimated base on the takahashi [23]correlation that given the diffusion coefficient at a given temperature and pressure, extrapolates to the intended operating conditions. To estimate the low pressure value of the coefficient the Fuller method [23] has been used:

$$D_{AB} = \frac{0.00143T^{1.75}}{PM_{AB}{}^{0.5}\left[(\sum v)_A^{1/3} + (\sum v)_B^{1/3}\right]^2}$$

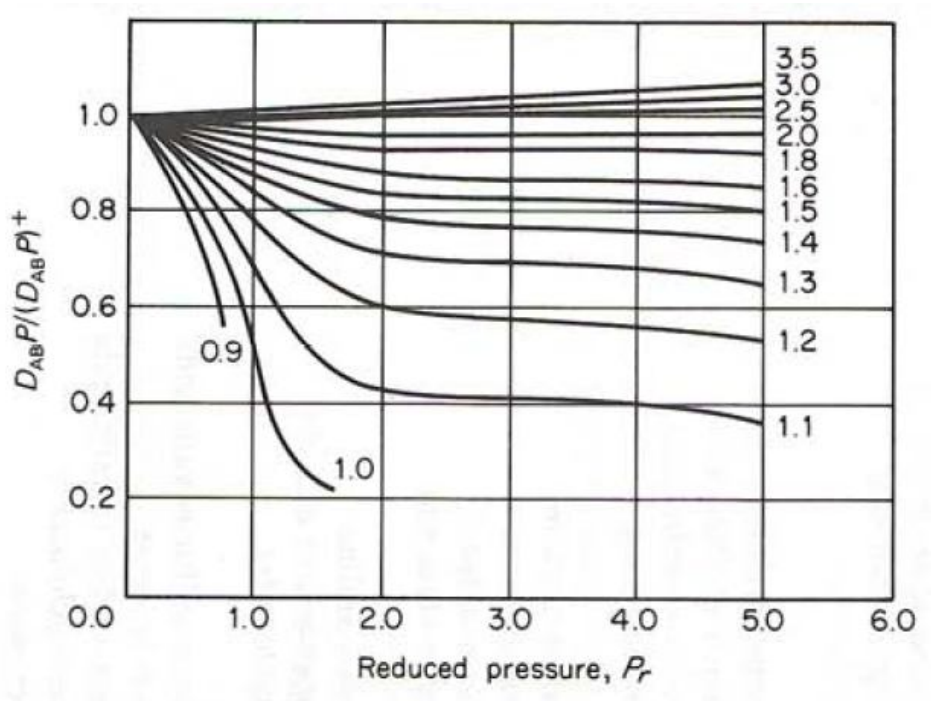

Figure H1. Takahashi correlation for the effect of pressure and temperature on the binary diffusin coefficient

Table H1. Estimated values for the low pressure diffusion coefficient and for 250 bar

						Fuller's method	Takhahashi correlation
Run	Temperature (ºC)	Pressure (bar)	Tr	Pr	$D_{AB}P$ / $(D_{AB}P)^+$	$(D_{AB})^+$ at 1 bar (cm2/s)	(D_{AB}) at 250 bar (cm2/s)
1	150	250	1,000	10,9	0,600	$9,6799x10^{-4}$	$2,3232\ x10^{-6}$
2	150	250	1,000	10,9	0,600	$9,6799\ x10^{-4}$	$2,3232\ x10^{-6}$
3	150	250	1,000	10,9	0,600	$9,6799\ x10^{-4}$	2,3232E $x10^{-6}$
4	150	250	1,000	10,9	0,600	$9,6799\ x10^{-4}$	2,3232E- $x10^{-6}$
5	180	250	1,071	10,9	0,700	$1,0913\ x10^{-3}$	3,0555E $x10^{-6}$
6	180	250	1,071	10,9	0,700	$1,0913\ x10^{-3}$	3,0555E $x10^{-6}$
7	180	250	1,071	10,9	0,700	$1,0913\ x10^{-3}$	3,0555E $x10^{-6}$
8	180	250	1,071	10,9	0,700	1,0913E $x10^{-3}$	3,0555E $x10^{-6}$
9	205	250	1,130	10,9	0,720	1,1988E $x10^{-3}$	3,4525E $x10^{-6}$
10	205	250	1,130	10,9	0,720	1,1988E $x10^{-3}$	3,4525E $x10^{-6}$
11	205	250	1,130	10,9	0,720	1,1988E $x10^{-3}$	3,4525E $x10^{-6}$
12	205	250	1,130	10,9	0,720	1,1988E $x10^{-3}$	3,4525E $x10^{-6}$

H. Kinetic Analysis

The following pictures were taken directly from Matlab, and present the concentration profiles for 150 and 180ºC.

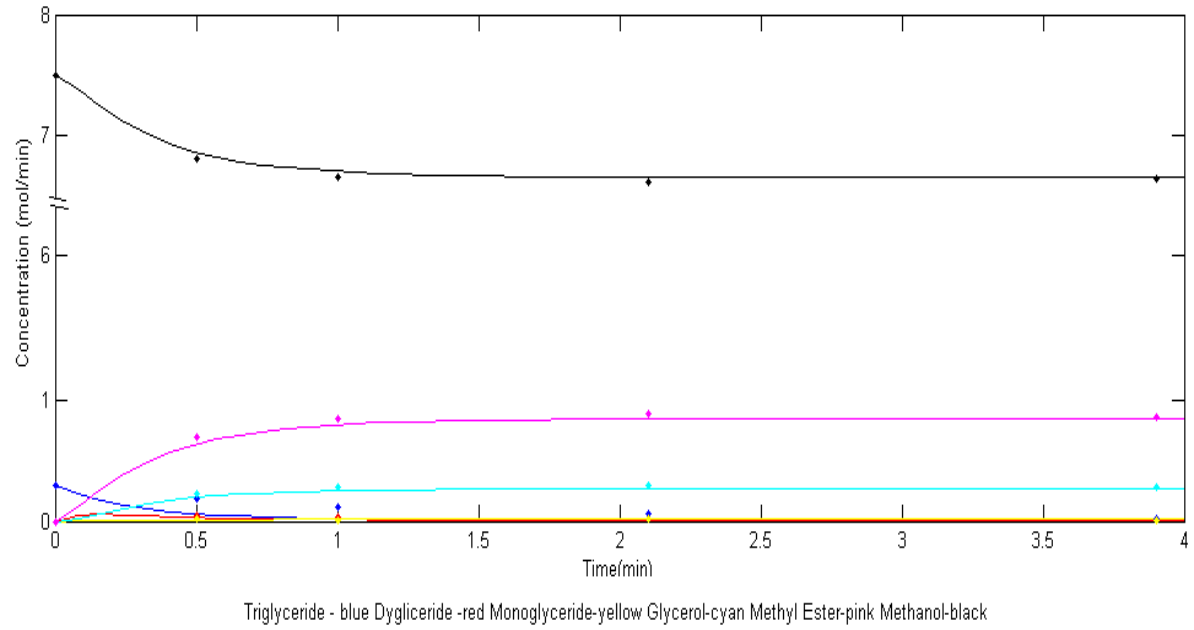

Figure I1. Content of methyl esters, triglycerides, diglycerides, monoglycerides, glycerol and methanol in the products obtained at 180ºC, 250 bar, catalyst mass of 9g, and methanol/oil ratio of 25.

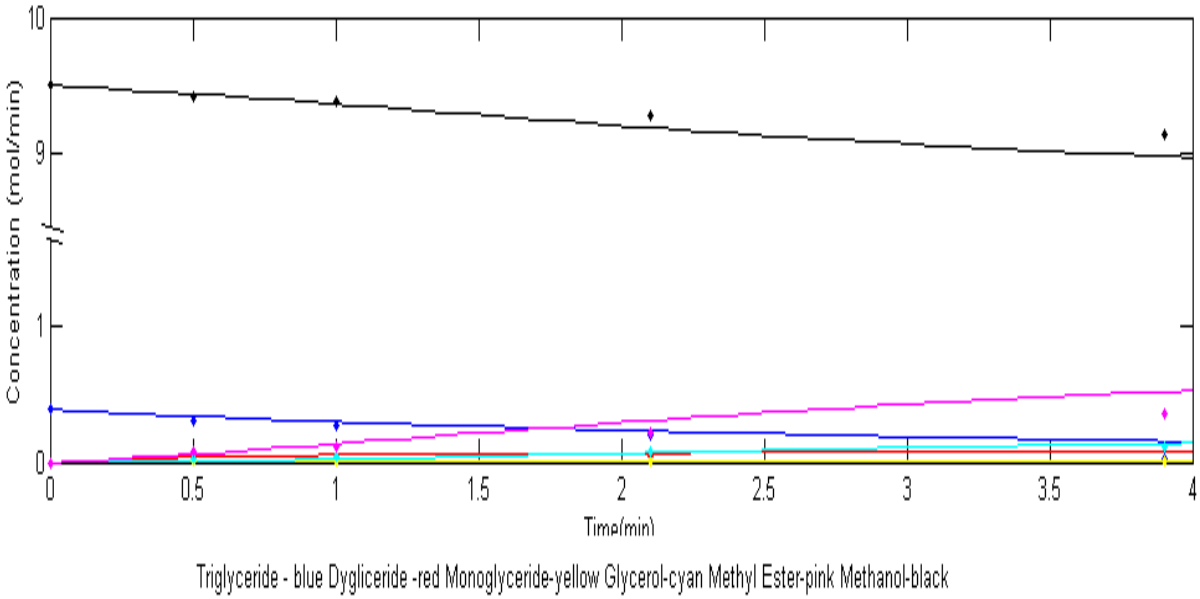

Figure I2. Content of methyl esters, triglycerides, diglycerides, monoglycerides, glycerol and methanol in the products obtained at 150ºC, 250 bar, catalyst mass of 9g, and methanol/oil ratio of 25.

In the following line is the Matlab code written and used for the adjust of the kinetic model to the experimental points.

```
% DERV Função executada por ode45.m com a descrição do sistema de equações
diferenciais
% t - posição onde calcular o valor das derivadas de Ci(t)
% C - vector com os valorer Ci(t)  na posição t
% flag - flags usadas pela função ode45.m
% k1, k2, k3, k4, k5, k6 - constantes cienticas do sistema diferencial
%Triglyceride-1
%Dygliceride -2
%Monogliceride-3
%Glycerol-4
%Methyl Ester -5
%Methanol -6
function dC=derv(t,C,flag,k1,k2,k3,k4,k5,k6)
dC(1)=0.5*(-k1*C(1)*C(6)+k2*C(5)*C(2));
dC(2)=0.5*(k1*C(1)*C(6)-k2*C(5)*C(2)-k3*C(2)*C(6)+k4*C(5)*C(3));
dC(3)=0.5*(k3*C(2)*C(6)-k4*C(5)*C(3)-k5*C(3)*C(6)+k6*C(5)*C(4));
dC(4)=0.5*(k5*C(3)*C(6)-k6*C(5)*C(4));
dC(5)=0.5*(k1*C(1)*C(6)-k2*C(2)*C(5)+k3*C(2)*C(6)-
k4*C(5)*C(3)+k5*C(3)*C(6)-k6*C(4)*C(5));
dC(6)=0.5*(-k1*C(1)*C(6)+k2*C(2)*C(5)-k3*C(2)*C(6)+k4*C(5)*C(3)-
k5*C(3)*C(6)+k6*C(4)*C(5));
dC=dC'; % Passagem do vector das derivadas de linha para coluna
end
```

```
%test de k's
%clear all
%clc
Cexp=[0.3 0.03702 0.02422 0.00238 0.00320;0 0.01759 0.01446 0.004444
0.00324;0 0.01545 0.01397 0.00898 0.00670;0 0.2142 0.2614 0.2731 0.26511;0
0.64270 0.78429 0.81944 0.79534;7.5 6.85730 6.71571 6.68056 6.70466];
Cexp=Cexp';
t1=[0 0.5 1 2.1 3.9];

k0=[1.5093;20.9368;3.1695;15.6845;249.3535;90.2957];

kLB=zeros(6,1);
kUB=ones(6,1)*500;


OF=perfilConcs(k0);
options = optimset('LargeScale','off','TolCon',1e-
16,'MaxFunEvals',10000,'TolFun',1e-18,'Display','iter');
kopt = fmincon(@perfilconcs,k0,[],[],[],[],kLB,kUB,[],options);

[t,C]=perfilConcs2(kopt);


plot(t,C(:,1),'b-',t,C(:,2),'r-',t,C(:,3),'y-',t,C(:,4),'c-',t,C(:,5),'m-
',t,C(:,6),'k-
```

```
',t1,Cexp(:,1),'b.',t1,Cexp(:,2),'r.',t1,Cexp(:,3),'y.',t1,Cexp(:,4),'c.',t
1,Cexp(:,5),'m.',t1,Cexp(:,6),'k.');% Gráfico de C(i)
xlabel('Time(min)')
ylabel('Concentration (mol/L)')
title('Triglyceride - blue Dygliceride -red Monoglyceride-yellow Glycerol-
cyan Methyl Ester-pink Methanol-black')
```

```
function [t,C]=perfilConcs2(k)

%k1 = 5;k2 = 0.001;k3 = 20.67;k4 = 0.018;k5=30;k6=0.0510; % Constantes
cineticas do sistema de equações
t=linspace(0,4,1200); % Vector distância onde t = 0 até t = xx com 120000
pontos
Cini=[0.3 0 0 0 0 7.5]; % Valores iniciais das variaveis Ci(t) no ponto t =
0

OPTIONS=odeset('AbsTol',1e-10,'RelTol',1e-10); % Alteração do valor da
tolerância do

% método de RUNGE-KUTTA
% (função ODE45.m)
% Método de RUNGE-KUTTA. 'derv' é a função onde está descrito o sistema
diferencial
[t,C]=ode45('derv',t,Cini,OPTIONS,k(1),k(2),k(3),k(4),k(5),k(6));

Cexp=[0.3 0.03702 0.02422 0.00238 0.00320;0 0.01759 0.01446 0.004444
0.00324;0 0.01545 0.01397 0.00898 0.00670;0 0.2142 0.2614 0.2731 0.26511;0
0.64270 0.78429 0.81944 0.79534;7.5 6.85730 6.71571 6.68056 6.70466];
Cexp=Cexp';
end
```

```
function OF=perfilConcs(k)

%k1 = 5;k2 = 0.001;k3 = 20.67;k4 = 0.018;k5=30;k6=0.0510; % Constantes
cineticas do sistema de equações
t=linspace(0,4,1200); % Vector distância onde t = 0 até t = xx com 120000
pontos
Cini=[0.3 0 0 0 0 7.5]; % Valores iniciais das variaveis Ci(t) no ponto t =
0

OPTIONS=odeset('AbsTol',1e-10,'RelTol',1e-10); % Alteração do valor da
tolerância do

% método de RUNGE-KUTTA
% (função ODE45.m)
% Método de RUNGE-KUTTA. 'derv' é a função onde está descrito o sistema
diferencial
[t,C]=ode45('derv',t,Cini,OPTIONS,k(1),k(2),k(3),k(4),k(5),k(6));
```

```
Cexp=[0.3 0.03702 0.02422 0.00238 0.00320;0 0.01759 0.01446 0.004444
0.00324;0 0.01545 0.01397 0.00898 0.00670;0 0.2142 0.2614 0.2731 0.26511;0
0.64270 0.78429 0.81944 0.79534;7.5 6.85730 6.71571 6.68056 6.70466];
Cexp=Cexp';
t1=[0 0.5 1 2.1 3.9];


yModeloT=[];
for i=1:6
    yModelo=interp1(t,C(:,i),t1)';
    yModeloT=[yModeloT yModelo];
end

matdifs=(yModeloT-Cexp).^2;
weights=[100 500 1000 33 10 1];
OF=sum(sum(matdifs).*weights);
end
```

H- Mixture Methanol/CO_2 certificate of analysis

THE LINDE GROUP

Linde

HiQ®. Certificate.

Cliente / Costumer Name
UPC- ESTSEB ING. QUIMICA

Pavelló G Planta 2 Campus Sud Avda Diago
08028 Barcelona
España

Fecha de emisión / Date of issue 19/05/2010
Certificado n.°/ Certificate no. 5369
Botella n.° / Cylinder no. 416725
Código de artículo / Article code 2921
Cuest n.° / Order number NE - 601
Pagina n.° / Page number 1 (de / of 1)

Certificado de Análisis - Certificate of analysis

ISO 6141

Botella / Cylinder

Tipo de botella / Cylinder	Válvula / Cylinder connectio	Presión de llenado / Cylinder pressure (15°C)	Contenido Contents
Aluminio-20	Laton SVR-DIN 477 No.14	40 bar	14,7 kg

Componente / Component		Pedido / Ordered	Resultado analítico/ Analysis result	Incertidumbre/ Uncertainty	Unidad (Volumen)/ Unit (Volume)
METANOL / METHANOL	CH3OH	= 25	= 24,84	± 0,25	peso-%
DIOXIDO DE CARBONO / CARBON DIOXIDE	CO2	= Resto/bal.			

Nivel de confianza / Confidence level: 95 % k=2
Tolerancia de preparación / Blend tolerance: N/A
Temperatura mínima de almacenamiento y uso
Recommended storage and usage temperature: 0°C a / to +40°C
Presión mínima de utilización / Min. utilization pressure: 5 % del contenido real / of actual contents
Utilizar antes de / Use before (DD-MM-YYYY): 18-05-2012
Comentarios / Comments: Valores gravimétricos

Los valores expresados en porcentajes y ppm deben interpretarse como partes por volumen ideal (= partes por mol). Todos los valores expresados en volumen se refieren a las condiciones STP (1013 hPa, 273.15K) /
Indications in percent and ppm are to be interpreted as ideal parts per volume (= amount of substance). All indications of volume are related to STP (1013 hPa, 273.15K)

100000 Pa = 1 bar, 273,15 K = 0° C

Local de producción / Production Site: Laboratorio de Gases Especiales, Rubí

Responsable del análisis / Responsible for the analysis:

AR

Abelló Linde, S.A. - Laboratorio
Pol. Ind. Rubí Sur - Sub. 3, Av. Gaudí, 151
08191 Rubí (Barcelona)

HiQ® Certificate

Abelló Linde, S.A.
Rubí, 135 - 08009 Barcelona
Tel. +34 93 476 74 00, Fax + 34 93 207 57 64
www.abello-linde-sa.es

Laboratorio de Gases Especial
Pol. Ind. Can Pi de Vilaroch - Rubí Sur
Avda. Antoni Gaudí, 151
08191 Rubí (Barcelona), Spain